Astrofisica Nucleare e Subnucleare

Gamma ray Bursts – II

The Compton Gamma Ray Observatory

http://cossc.gsfc.nasa.gov

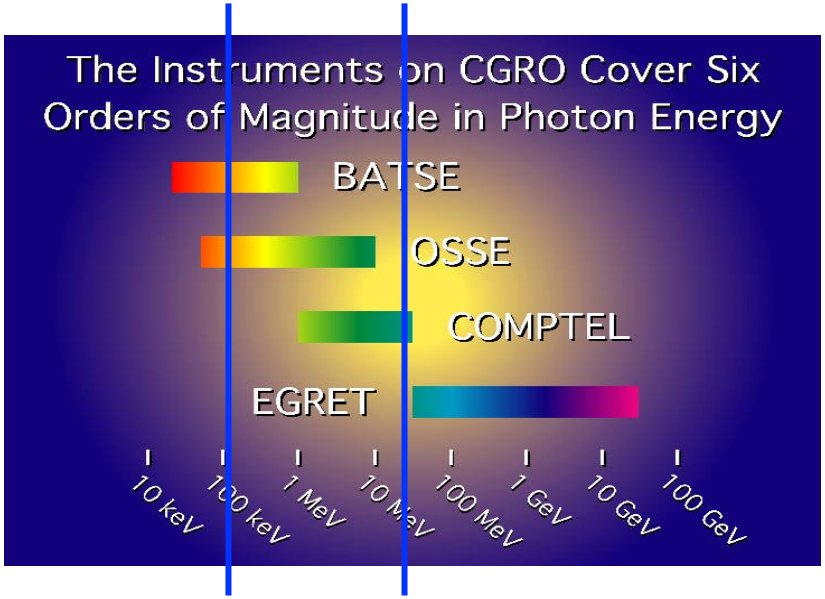

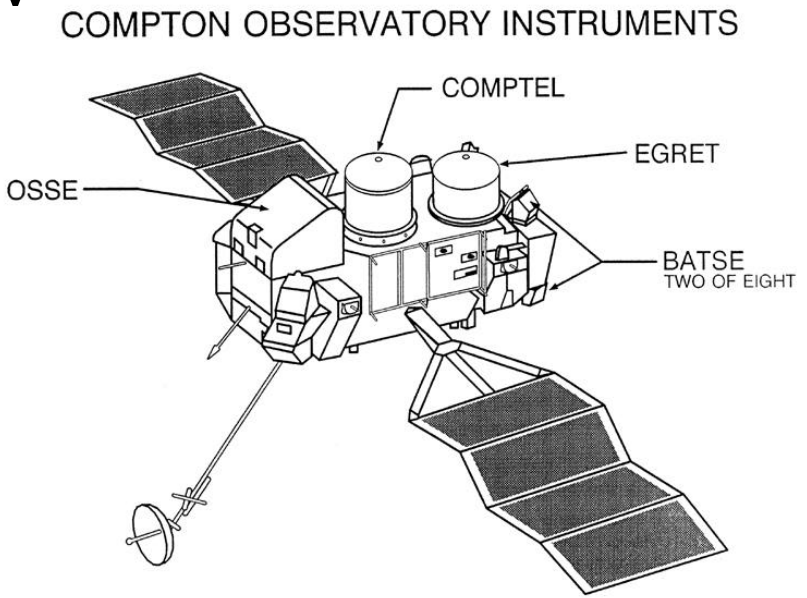

The Compton Gamma Ray Observatory (CGRO) is a sophisticated satellite observatory dedicated to observing the high-energy Universe. It is the second in NASA's program of orbiting "Great Observatories", following the Hubble Space Telescope.
While Hubble's instruments operate at visible and ultraviolet wavelengths, Compton carries a collection of four instruments which together can detect an unprecedented broad range of high-energy radiation called gamma rays. These instruments are the Burst And Transient Source Experiment (BATSE), the Oriented Scintillation Spectrometer Experiment (OSSE), the Imaging Compton Telescope (COMPTEL), and the Energetic Gamma Ray Experiment Telescope (EGRET).

The Compton Gamma Ray Observatory

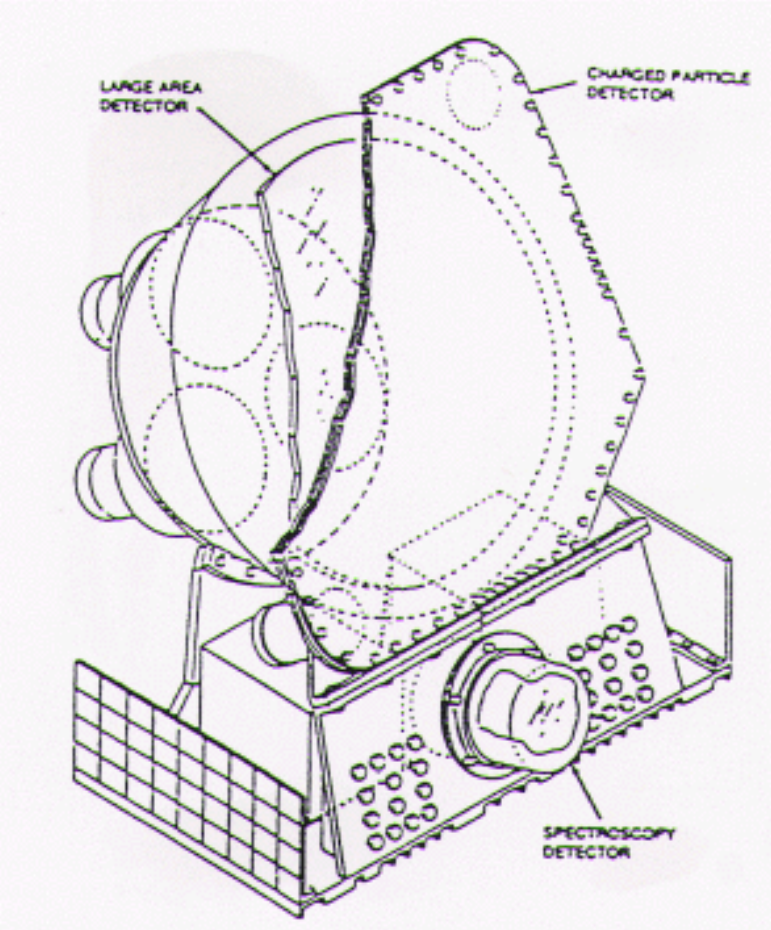

BATSE

- 20 keV -10 MeV
- GRB, SGR, X-ray sources

The Compton Gamma Ray Observatory

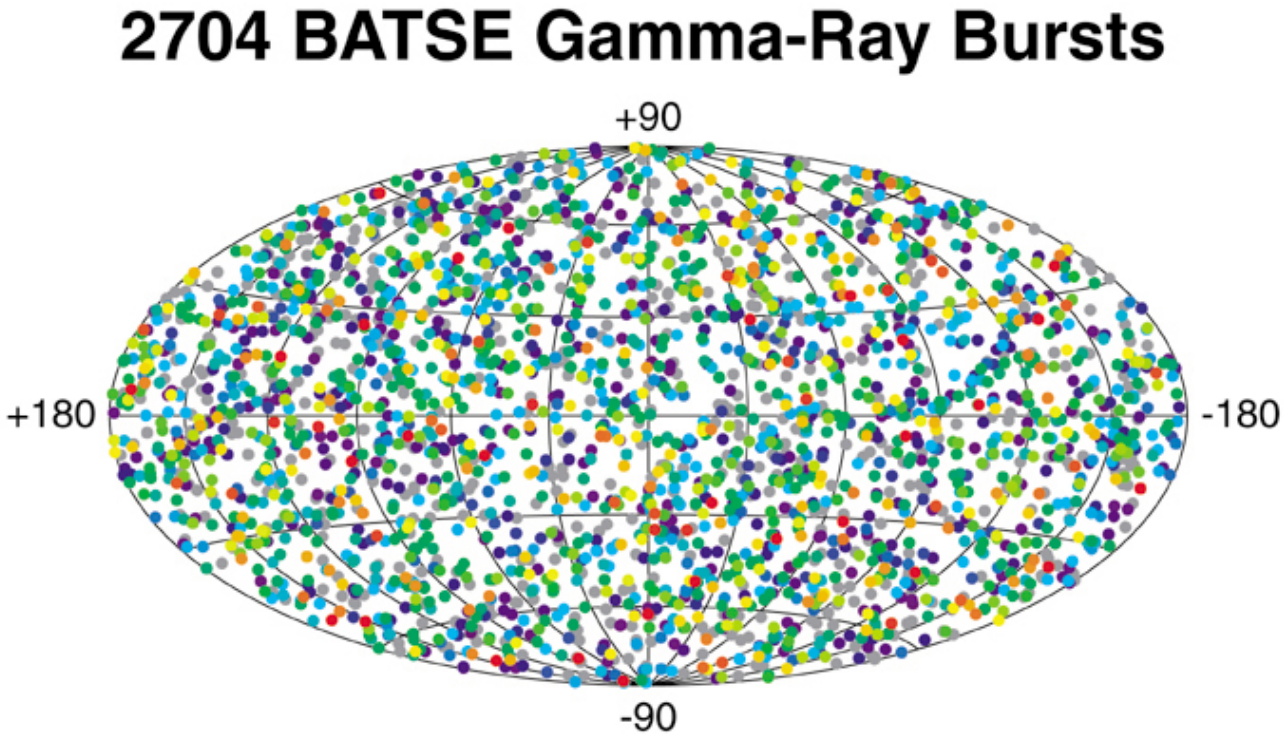

BATSE can determine directions to gamma-ray bursts with an accuracy of a few degrees. This diagram shows the positions of 2704 bursts detected with BATSE over 9 years of operation. The map is an Aitoff equal-area projection in Galactic coordinates. The only anisotropy detectable in the distribution is due to a small anisotropy in BATSE's sky exposure. The isotropic source distribution, combined with information from the burst intensity distribution, showed conclusively that the burst sources do not reside in the Galactic disk, as previously thought. This discovery initiated a paradigm shift to the view that the sources lie at cosmological distances. Direct redshift measurements have now confirmed this interpretation, making gamma-ray bursts the most powerful explosions in the Universe.

The Compton Gamma Ray Observatory

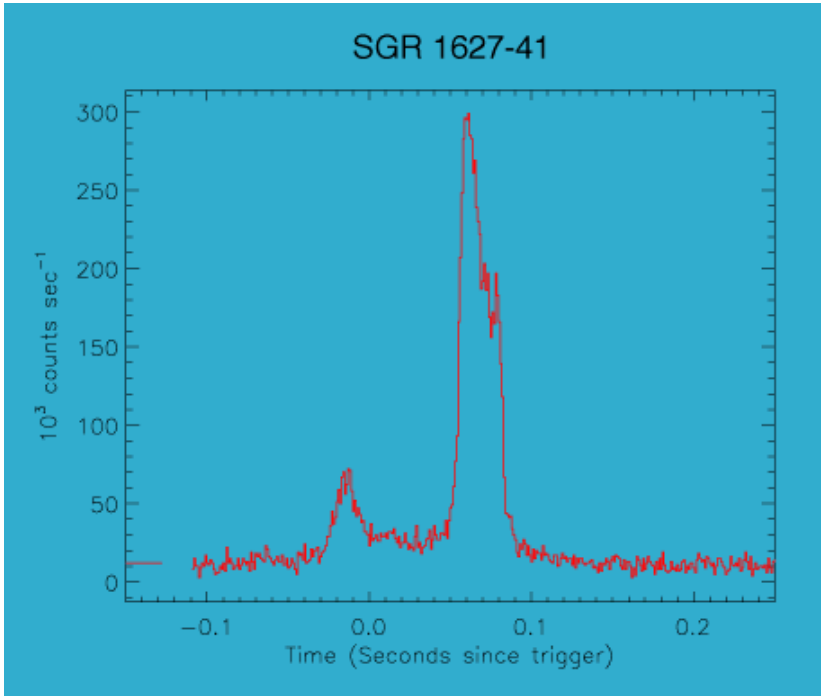

Soft Gamma Repeaters are one of the biggest success stories of BATSE on CGRO. These recurrent soft X-ray transients were discovered in the early '80s and identified as a separate population of young neutron stars that emitted frequent, but randomly spaced in time, outbursts of low-energy gamma rays, of very short duration, usually tenths of seconds. Until 1998 only three such sources were known; SGR 1627-41 is the first new SGR discovered with BATSE in June 1998. The figure displays a tremendous outburst from the source that reached a peak count rate of ~300000 counts s^{-1}, and lasted less than 150 ms. In 1998, SGRs were shown to possess extremely strong magnetic fields, of the order of 10^{14} Gauss, i.e., roughly 1000 times stronger than the average magnetic fields of radio pulsars and binary X-ray pulsars. They now form a well defined new class of objects, together with the Anomalous X-ray Pulsars (AXPs), called "magnetars".

The Compton Gamma Ray Observatory

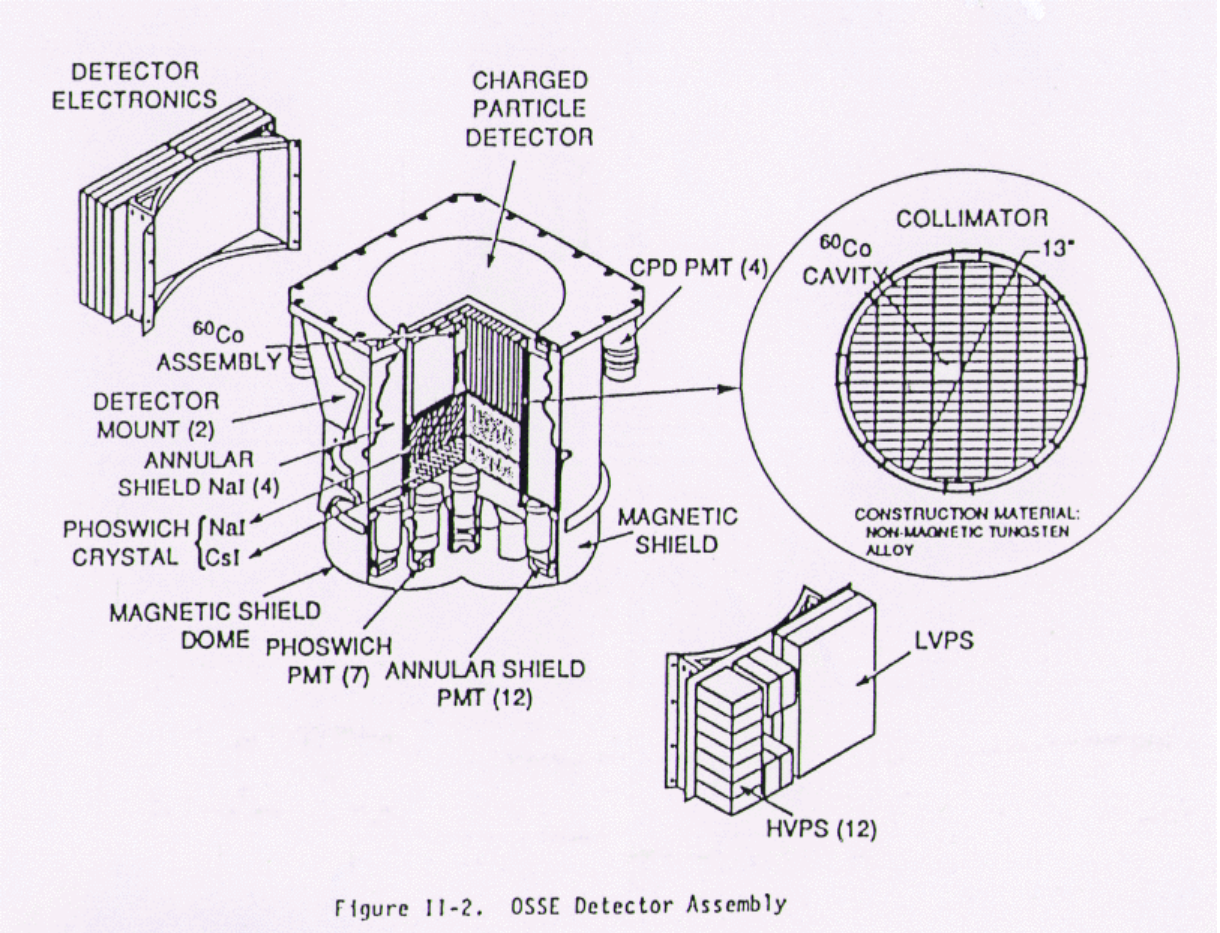

Figure II-2. OSSE Detector Assembly

OSSE

- 0.05-10 MeV
- e^+e^- annihilation, solar flares

OSSE detector

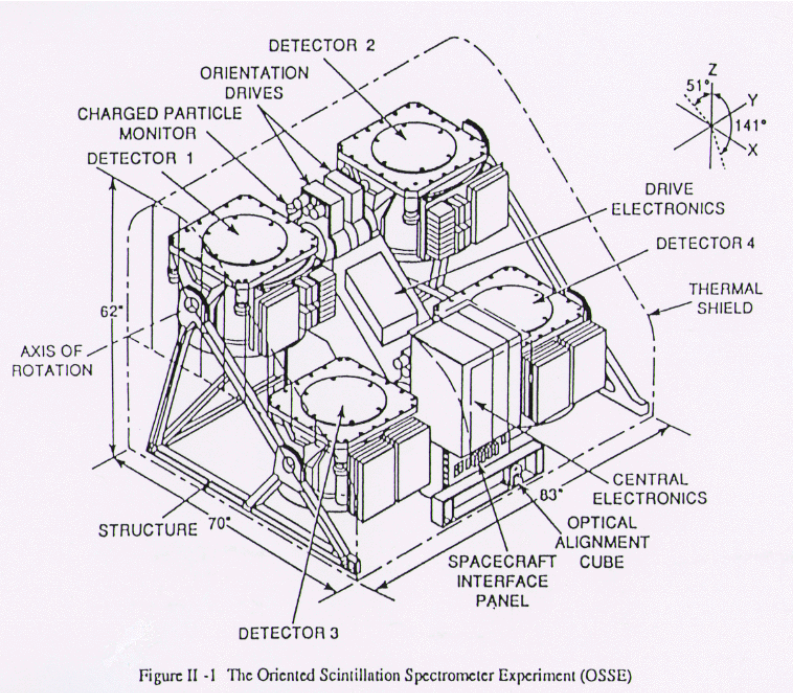

Figure II -1 The Oriented Scintillation Spectrometer Experiment (OSSE)

The Oriented Scintillation Spectrometer Experiment (OSSE) measured the distribution of the energy emitted from a number of gamma-ray sources, and as such studied nuclear lines in solar flares, radioactive decay of nuclei in supernova remnants, and matter-antimatter annihilation taking place near the center of our galaxy. OSSE consisted of four NaI scintillation crystals, and was sensitive to gamma rays with energies ranging from 50 keV to 10 Mev. Each of the detectors could be pointed individually. For most instances, observations of a gamma ray source were alternated with observations of nearby blank sky so as to be able to determine the background gamma ray emission.

The Compton Gamma Ray Observatory

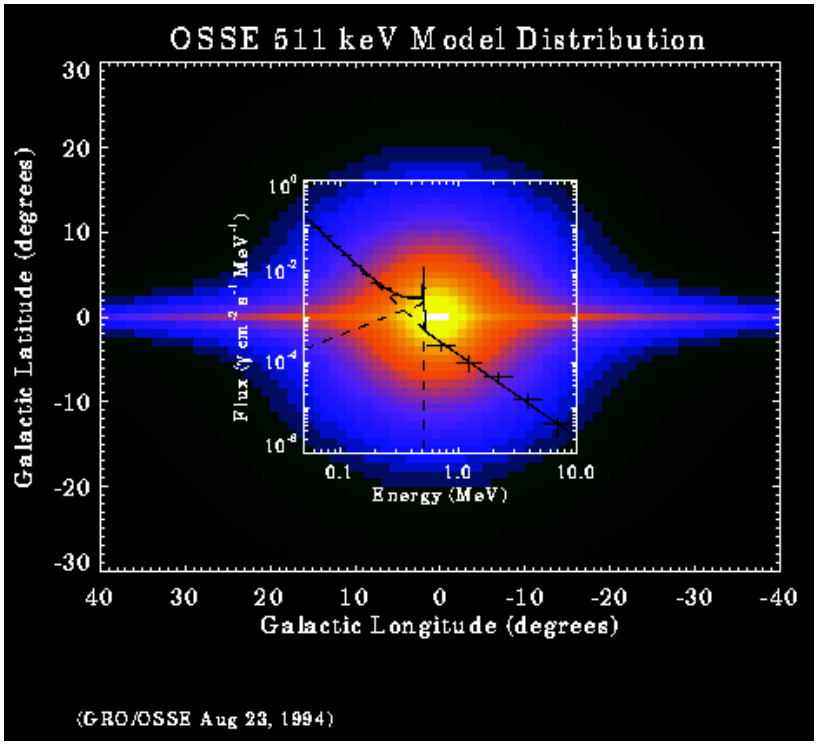

Intensity of gamma-ray emission from positron-electron annihilation in the plane of our Galaxy near the Galactic center. The emission is at 511 keV, which is the rest-mass energy of the electron and positron. The map is of a model that fits the OSSE 511 keV observations. OSSE has discovered that the radiation is mostly contained in a region of about 10 degrees diameter centered on the center of the Galaxy. The line plot superimposed on the map represents an OSSE observation of the 511 keV emission line.

The Compton Gamma Ray Observatory

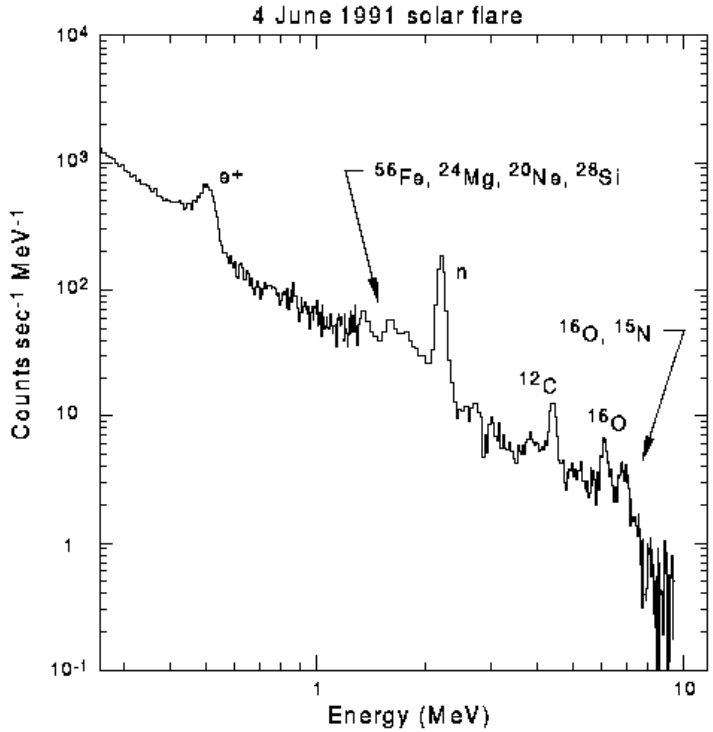

On June 4, 1991, the OSSE instrument observed a bright high-energy flare from an intensely active region of the sun. The energy spectrum of the flare shown in this slide indicates that solar flares accelerate particles to extremely high energies causing interactions which produce nuclear emission lines from excited atomic nuclei of Fe, Mg, Ne, Si, C, O, and N, along with emission lines from the formation of deuterium by neutron capture (labeled "n" in the slide) and electron-positron annihilation (labeled "e+").

Phoswich detectors

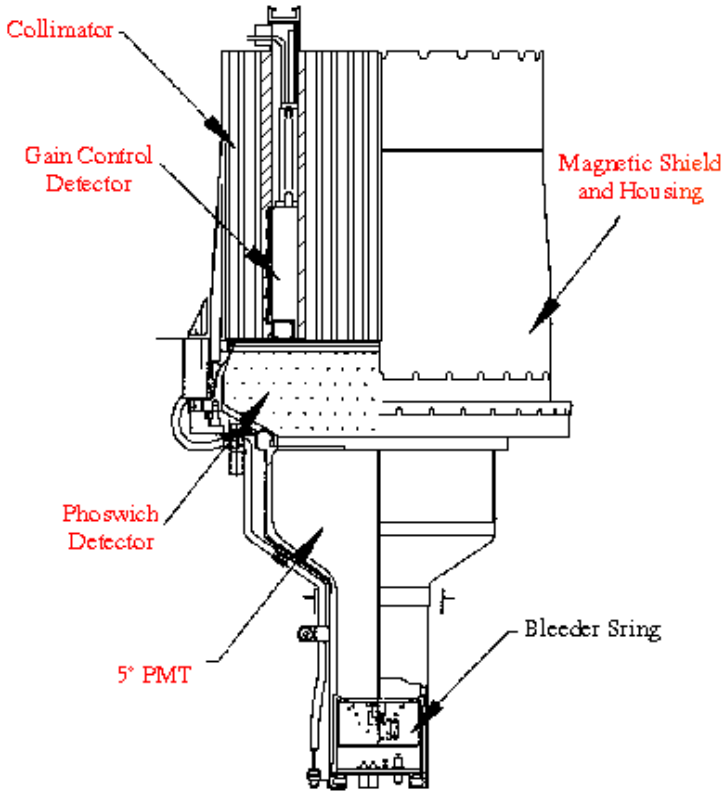

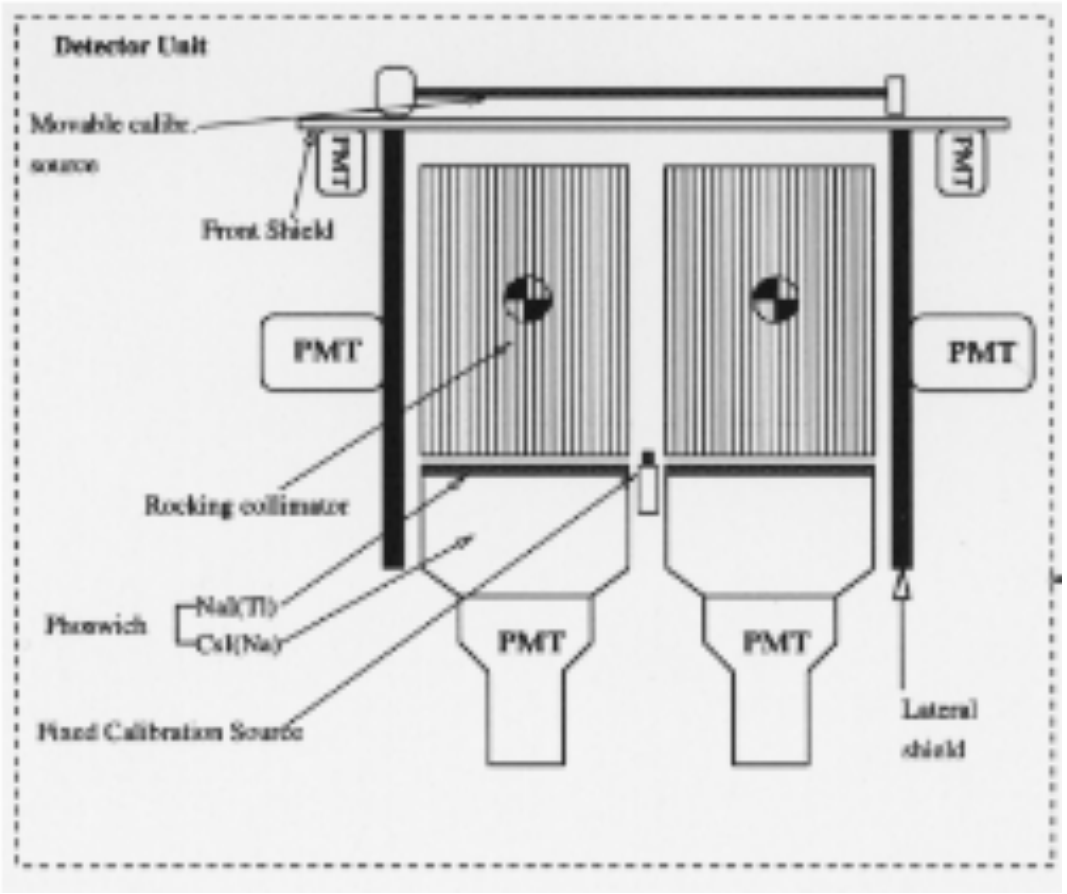

Two scintillators with different decay times. Pulse analysis can distinguish. Back scintillator used as shield at low energy, as detector at high energies.

Esempio: phoswich

The Phoswich (e.g. PDS on BeppoSAX)

Phoswich is short for 'phosphor sandwich'

Phosphor is the old name for a scintillator, and more than one are sandwiched together and viewed by the same photomultiplier.

More penetrating particles can produce signal in both scintillators

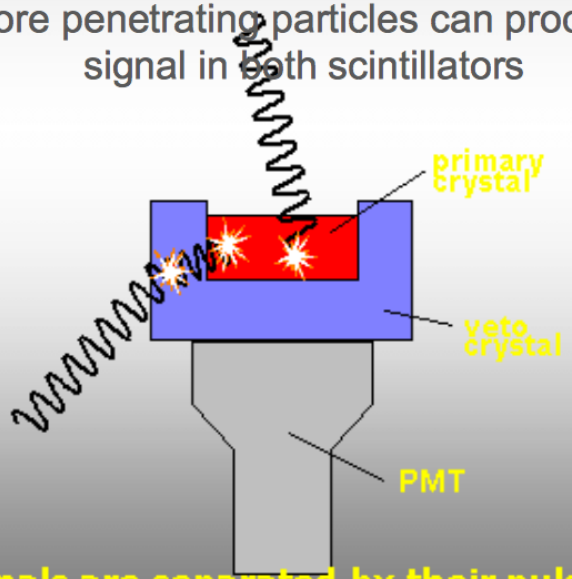

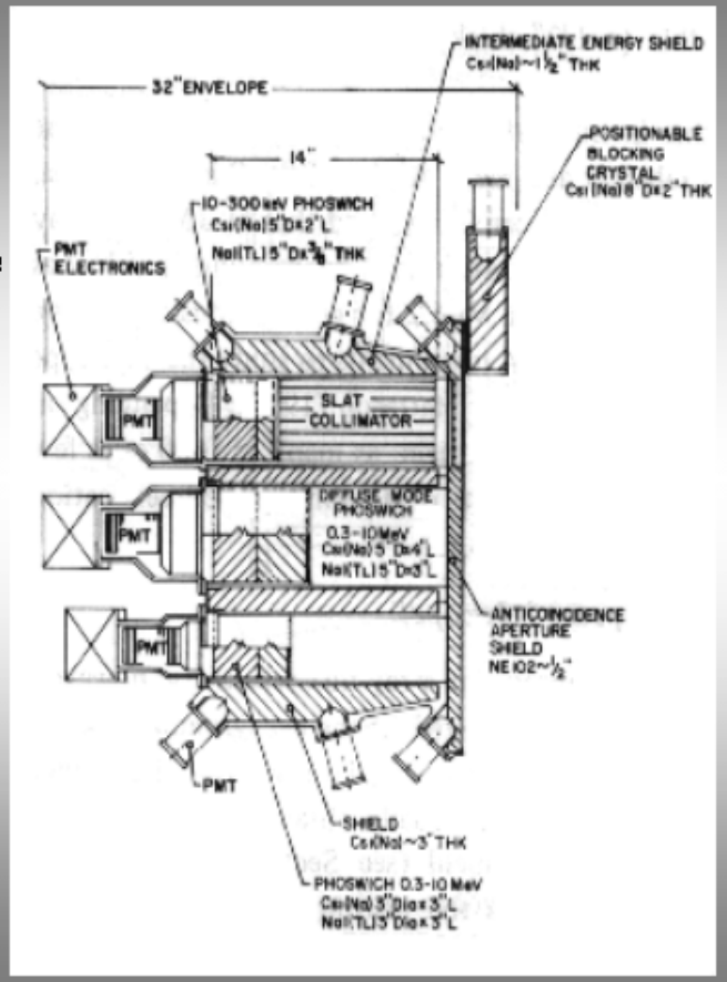

Signals are separated by their pulse shape

Different materials have different pulse shapes and are used to discriminate different events

BATSE (1991 - 2000)

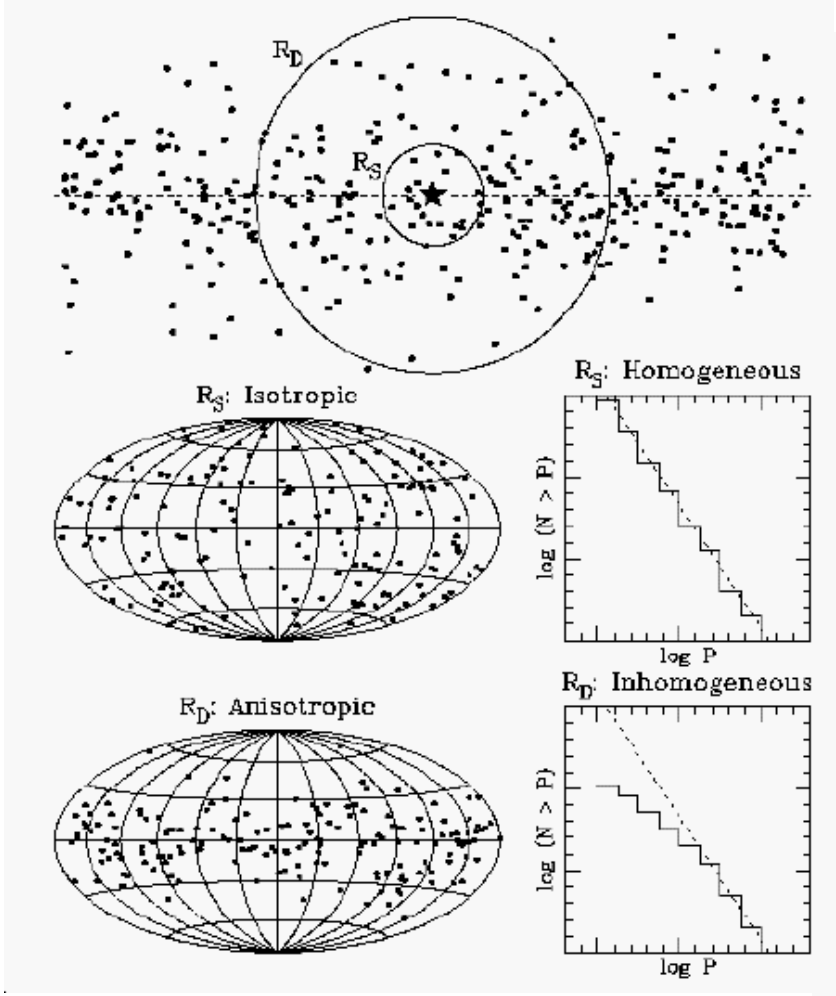

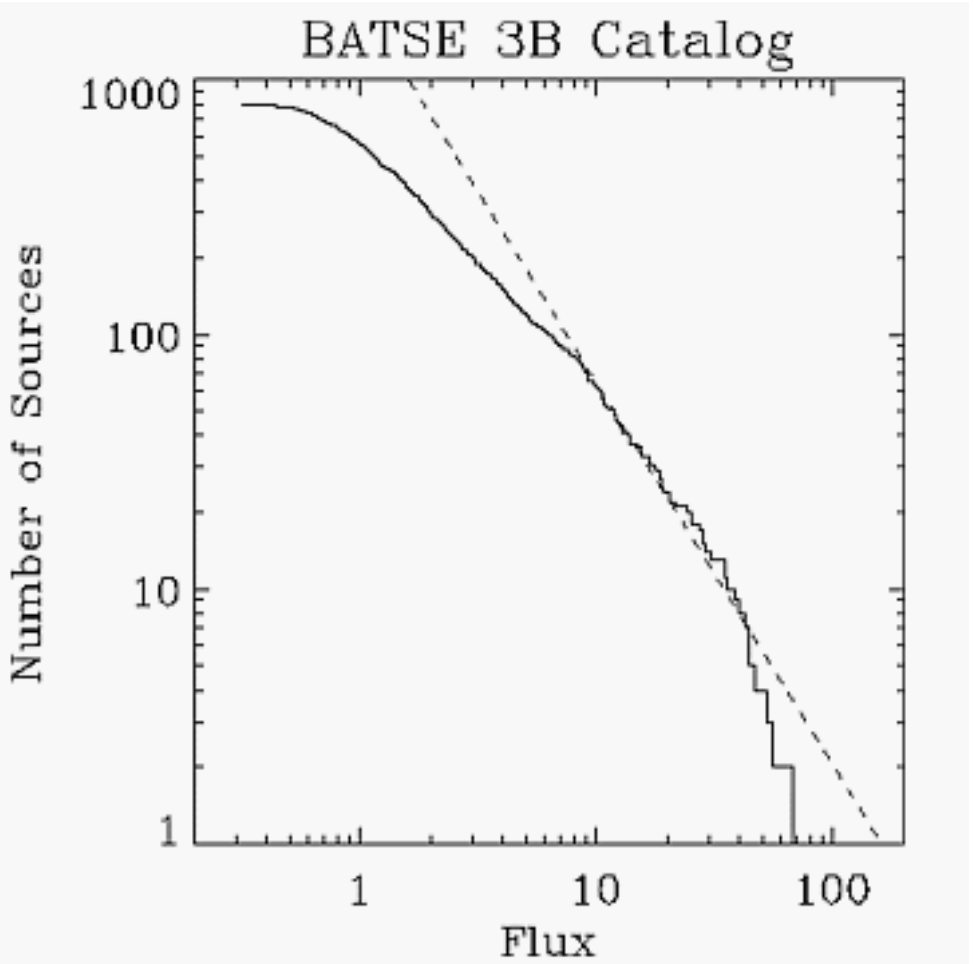

GRB: where are they?

The great debate (1995)

Cosmological - Galactic?

Flux: 10^{-7} erg cm^{-2} s^{-1}
Distance: 1 Gpc
Energy: 10^{51} erg

Distance: 100 kpc
Energy: 10^{43} erg

Need a new type of observation!

BeppoSAX (1995 - 2002)

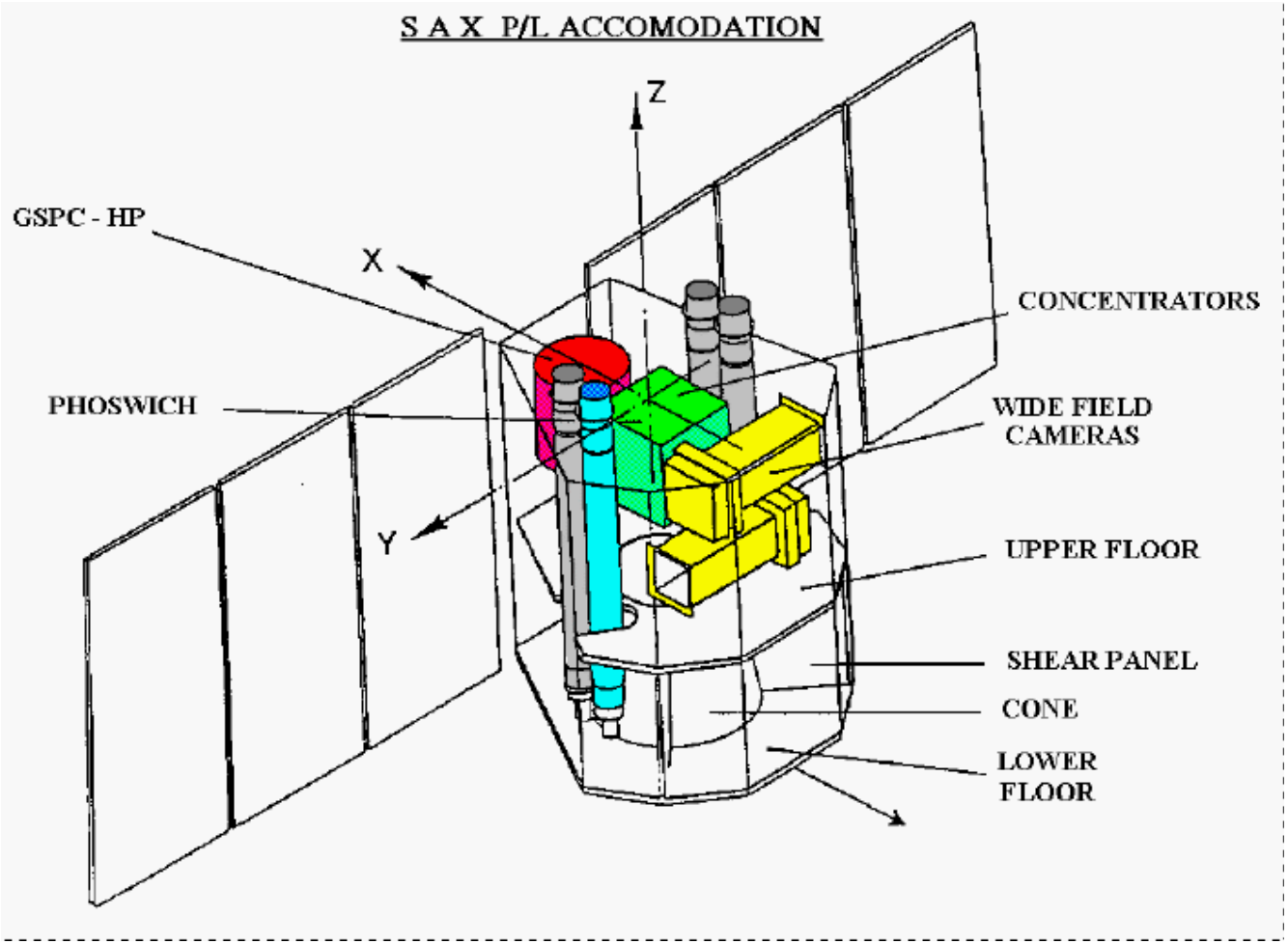

Spatial Aperture Modulation

- **Alternative to temporal modulation**
- **Requires two-dimensional position-sensitive detectors**
- **The spatial modulation is achieved by a pattern of holes in an otherwise absorbing plate, providing a unique spatial code**

Coded-aperture (or coded-mask) Telescopes

Principle: the mask pattern (in the form of the shadow produced by the parallel beam of an X-ray source) is recognized by the two-dimensional position-sensitive detector. Any shift in the pattern is related to a shift of the source position.

Coded Mask Imaging

The principle of the camera is straightforward: photons from a certain direction in the sky project the mask on the detector; this projection has the same coding as the mask pattern, but is shifted relative to the central position over a distance uniquely correspondent to the direction of the photons. The detector accumulates the sum of a number of shifted mask patterns.
Each shift encodes the position and its strength encodes the intensity of the sky at that position.

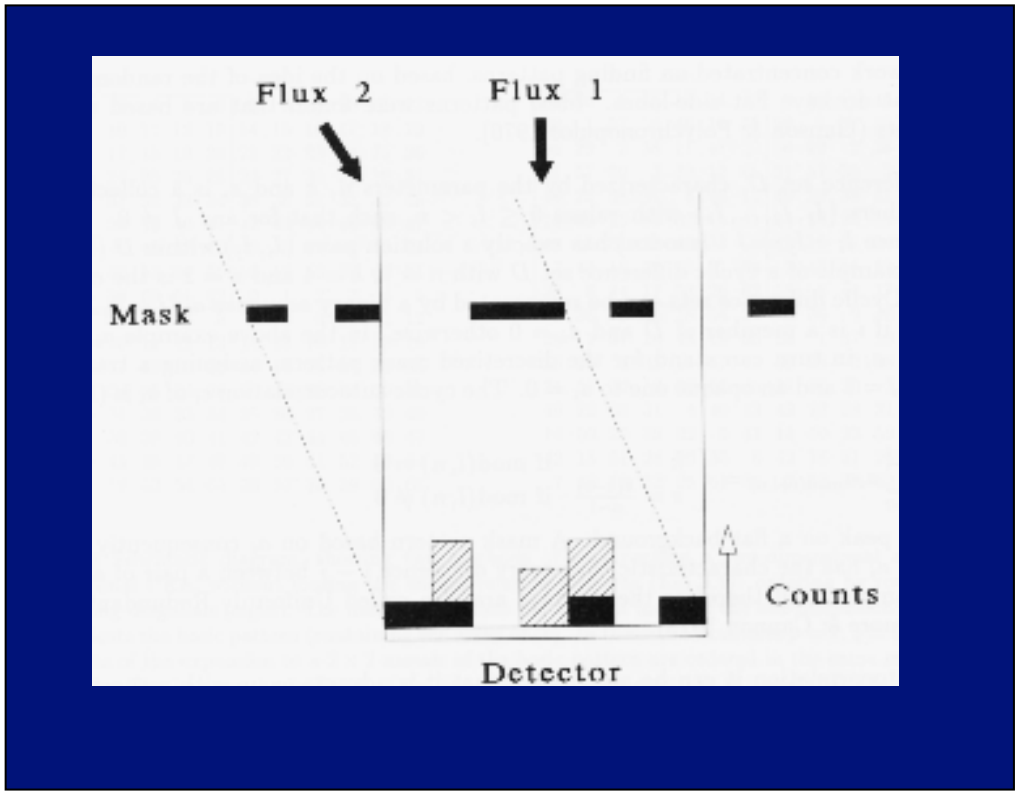

http://asd.gsfc.nasa.gov/archive/cai/coded_intr.html

Coded Mask Imaging

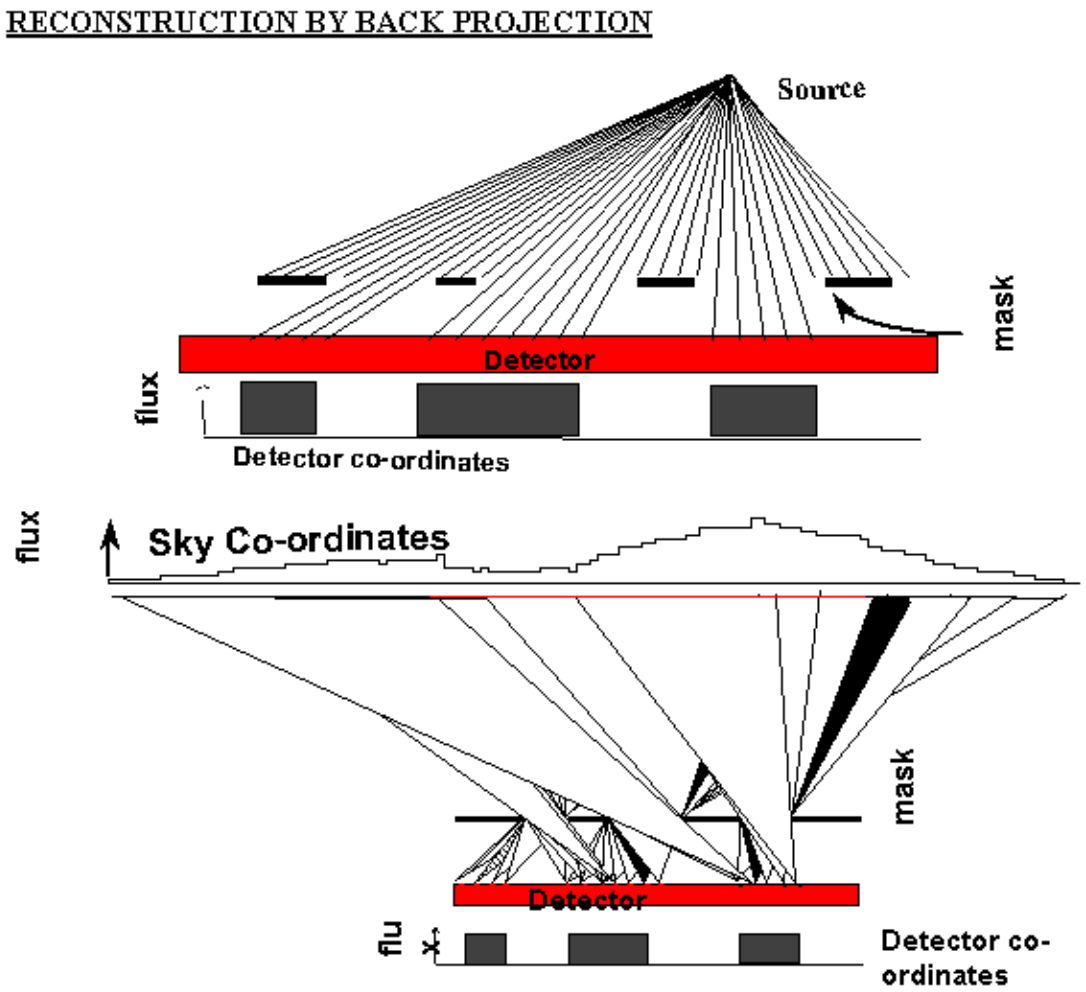

Coded Mask Imaging

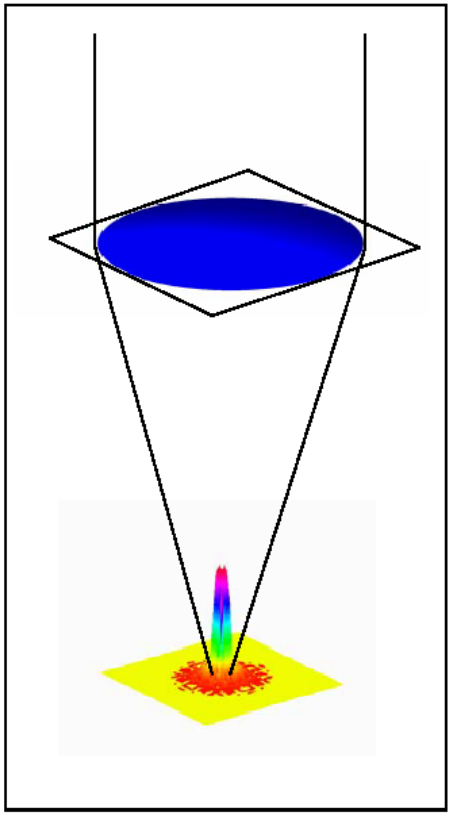

Point Source
Response
Function

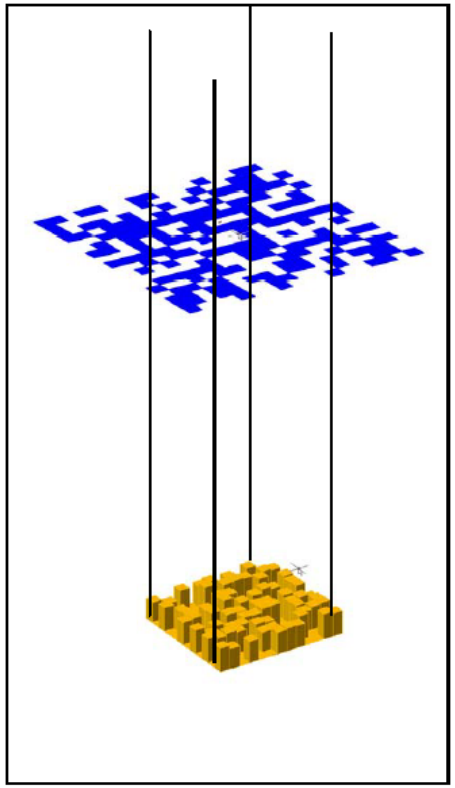

A coded mask telescope has the worst PSF imaginable

The response to a point source isn't just 'a bit blurred',

it fills the whole detector plane !

Coded Mask Imaging

'Optimum coded ' designs or 'URAs'

URAs are closely related to ' Cyclic Difference Sets '. Different families of cyclic difference sets yield Mask patterns which look quite different but which all have the desired properties - all have an ACF of the same form.

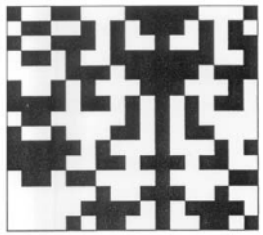

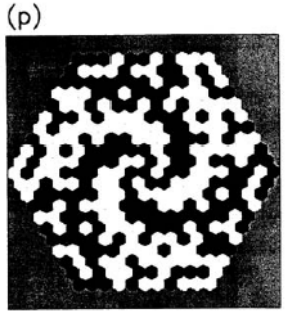

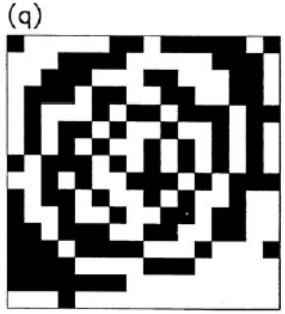

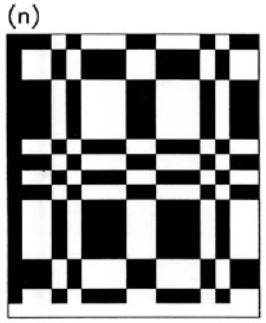

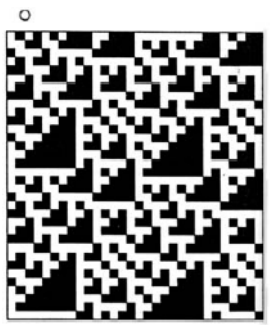

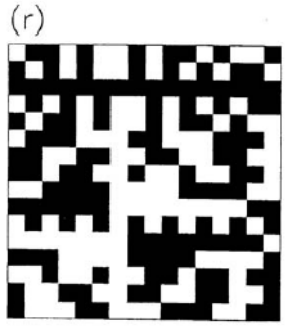

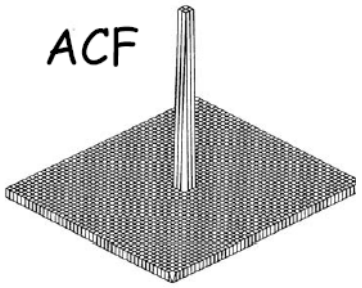

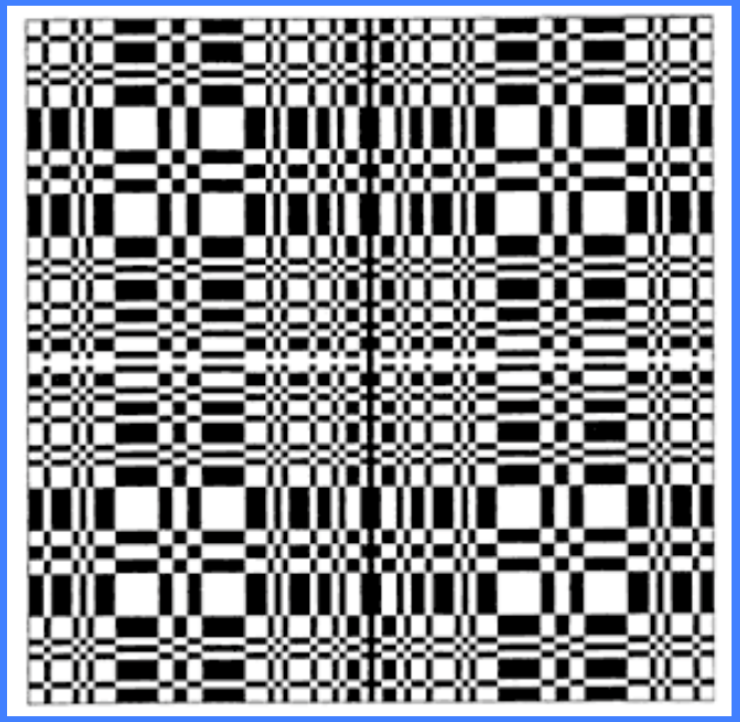

Mask of IBIS (15 keV – 10 MeV)
onboard *INTEGRAL*

Image Reconstruction

The observed intensity distribution over the detector must be interpreted ("unfolded") using the **coding function** associated with the mask pattern.

$$D(x)=M(x) \times S(x)$$

D(x)=observed detector distribution
M(x)=coding function (aperture modulation function)
S(x)=sky distribution
x=(X,Y) in the respective plane

D(x) must be inverted to get S(x)
S(x) not unambiguously defined, main problem coming from Poisson statistics because of the presence of background (often dominant over the source signal)

➔ $S(x)=B_{sky}(x)+sum(S_i(x))$ = X-ray background + all the i sources in the FoV, both coded by M(x)
+ detector background (charged particles, secondary photons)

M(x) directly inverted only for few mask patterns
Typically used *correlation procedures*=correlation of the aperture code with the suitably binned intensity distribution; *mismatched filtering*=FT^{-1} of the PSF; *backprojection*=the mask pattern is projected onto the sky, marking all areas from which the photon could have arrived.

The GRB phenomenon

- simultaneous detection of GRBs by GRBM and WFC

→ very accurate localization (few arcmin)

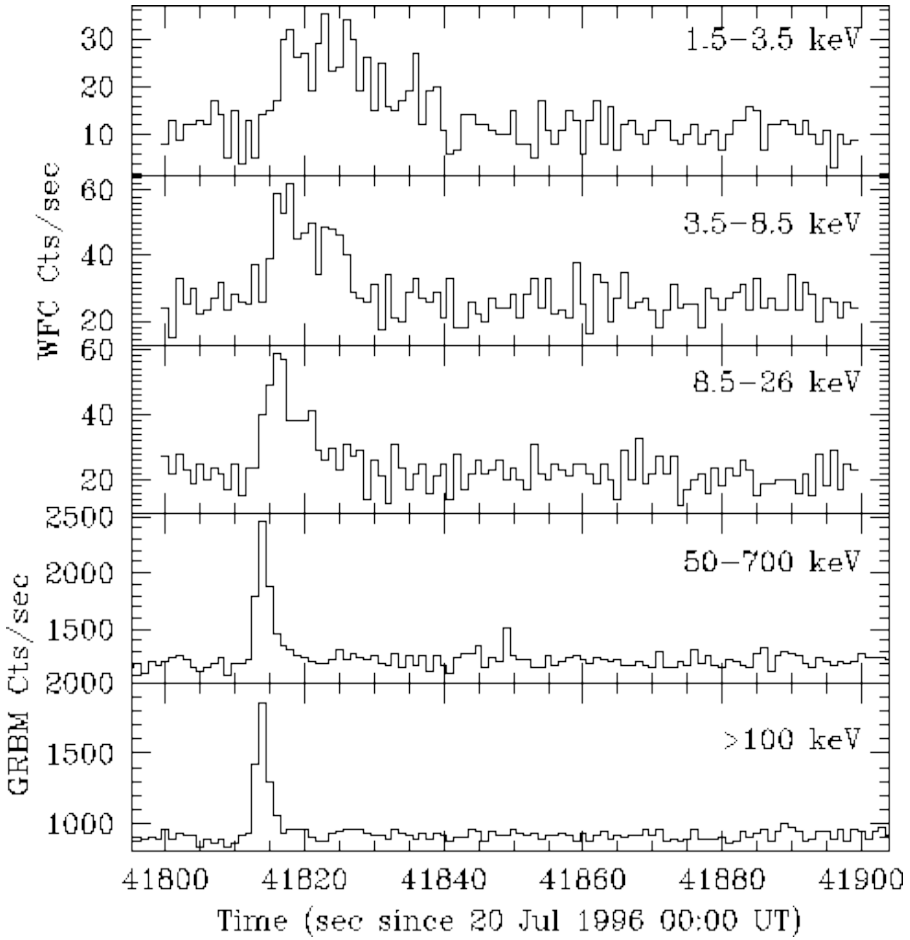

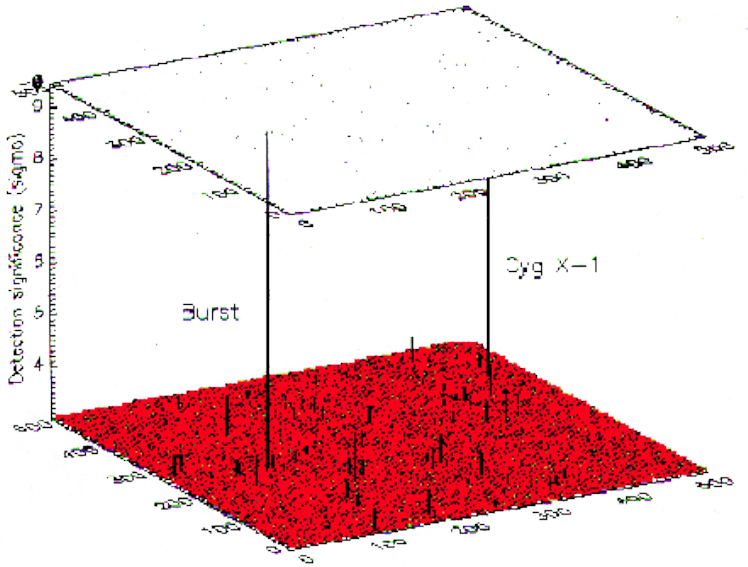

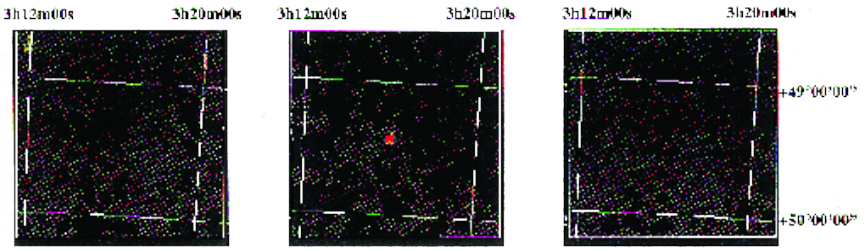

GRB960720, Piro et al., A&A, 1998

The GRB phenomenon

- in 1997, thanks to BeppoSAX observations, discovery of fading X-ray, optical, radio emission following the GRB

- photons received during the classical GRB phenomenon are then called "prompt emission" and the subsequent fading emission is called "afterglow emission"

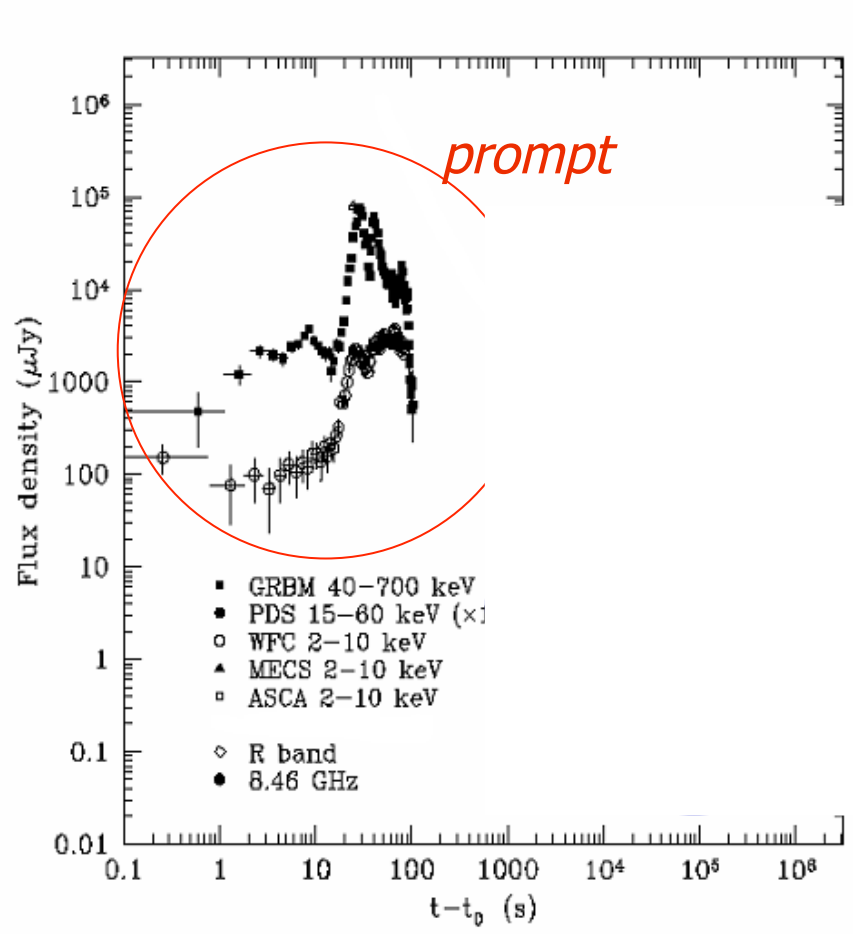

Adapted from Maiorano et al., A&A, 2005

GRB970228 – first good localization

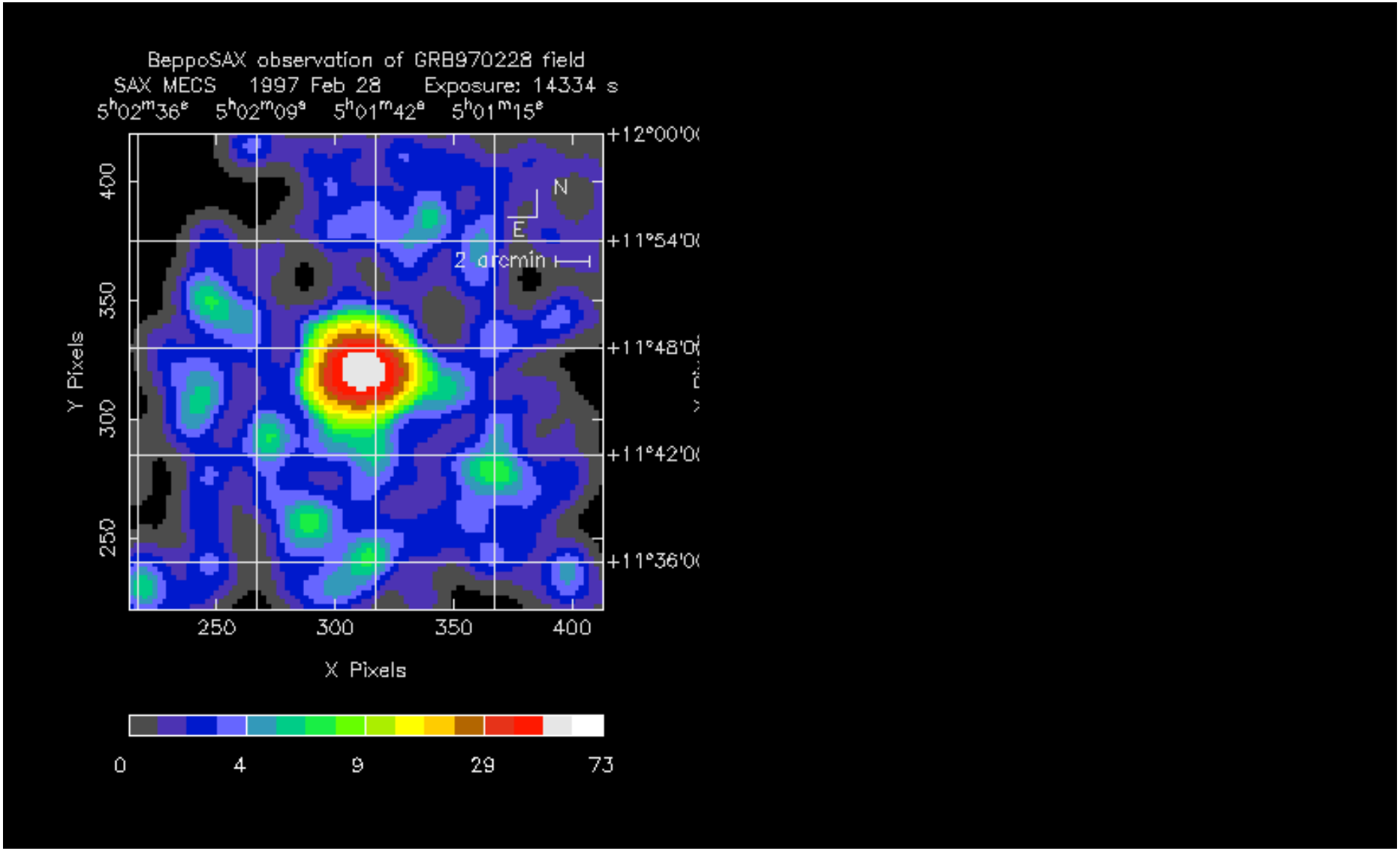

BeppoSAX

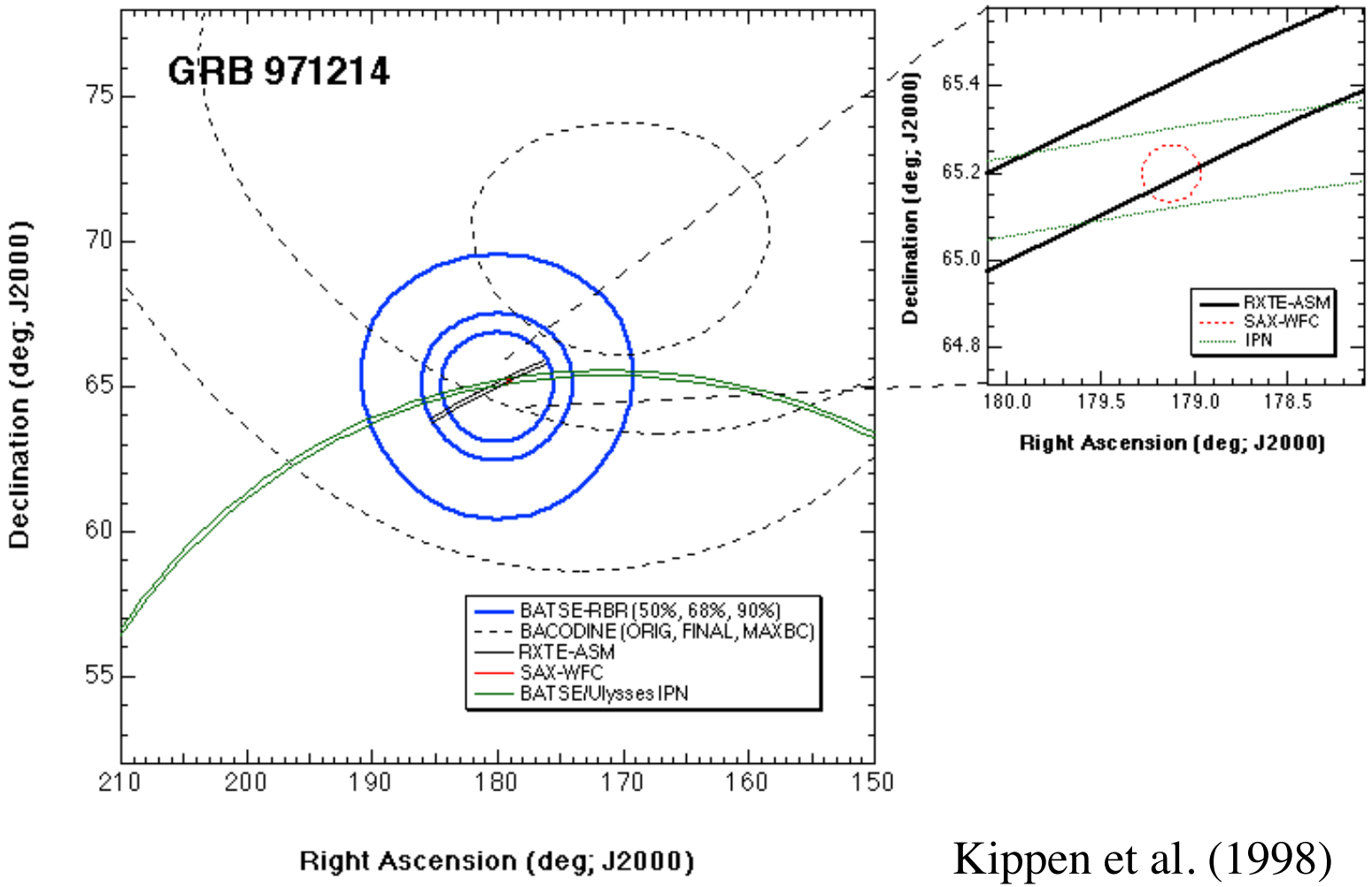

Kippen et al. (1998)

Afterglow Observations

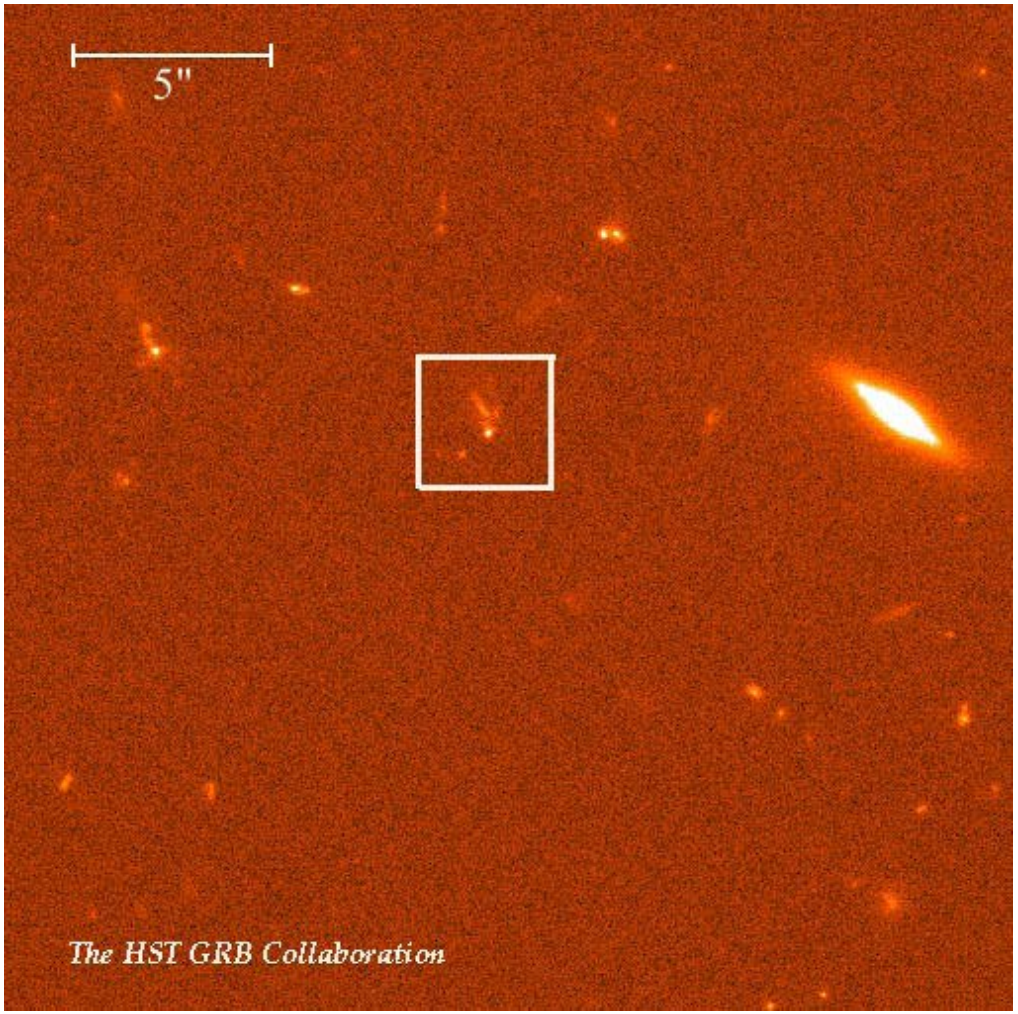

Identificazione delle Host Galaxies

Fruchter et al (1999)

The compactness problem

Light curve variability ~ 1 ms

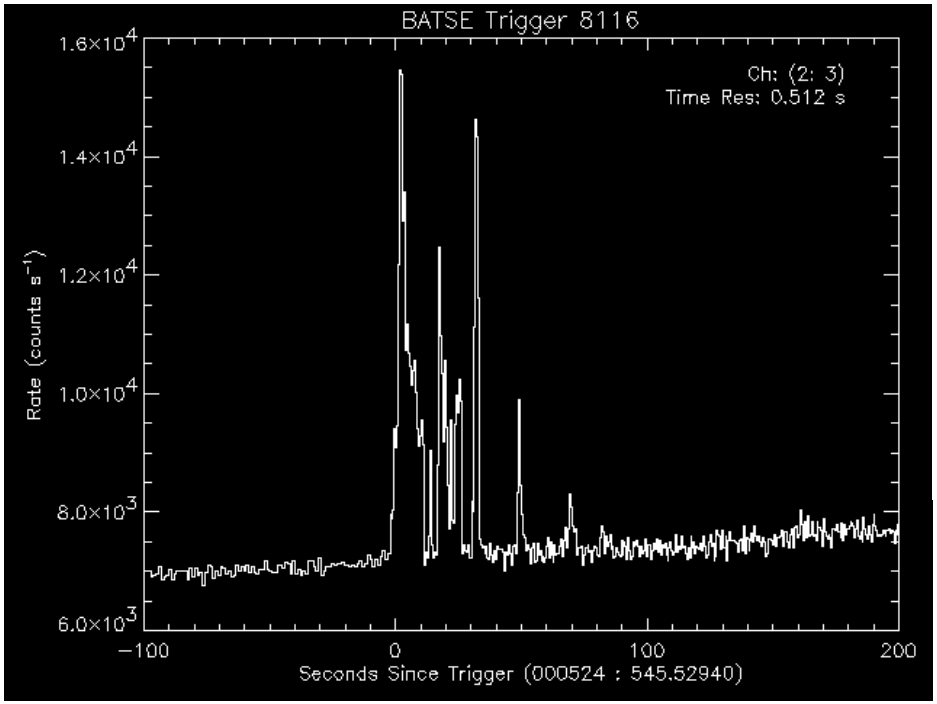

Briggs et al. (1999)

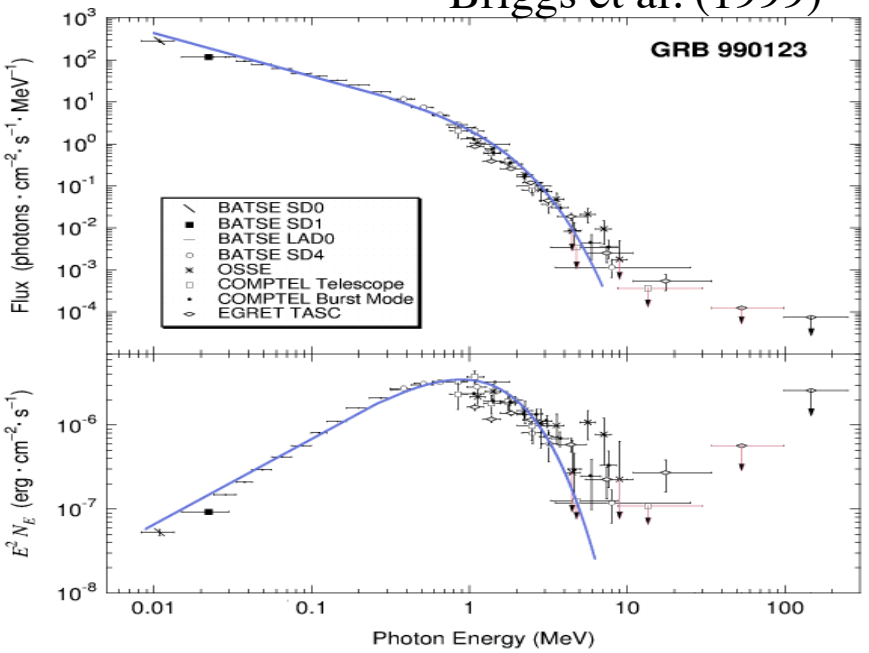

Non thermal spectra

- Fluence (γ): (0.1-10) x 10^{-6} erg/cm^2 ($\Omega/4\pi$)
- Total Energy: E ~ $10^{51} \div 10^{52}$ erg

Superluminal motion

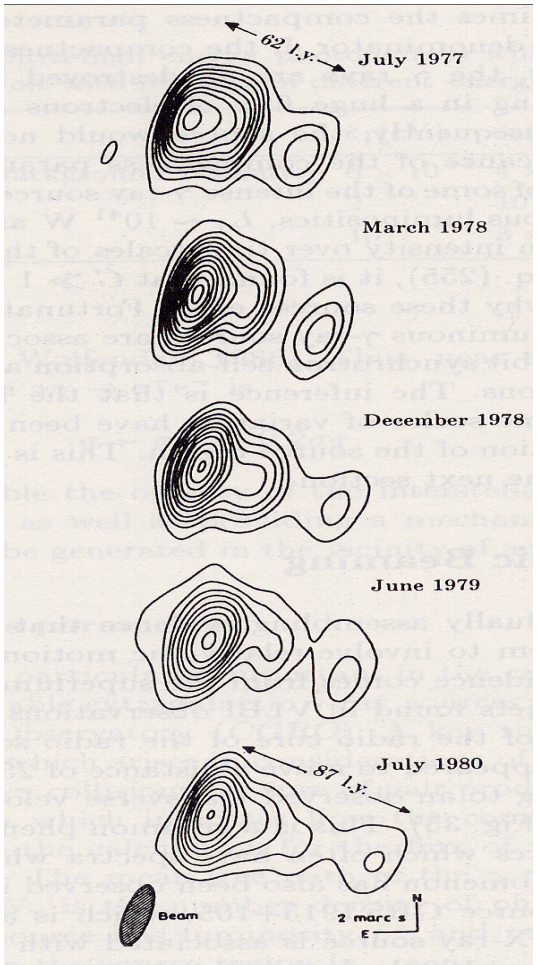

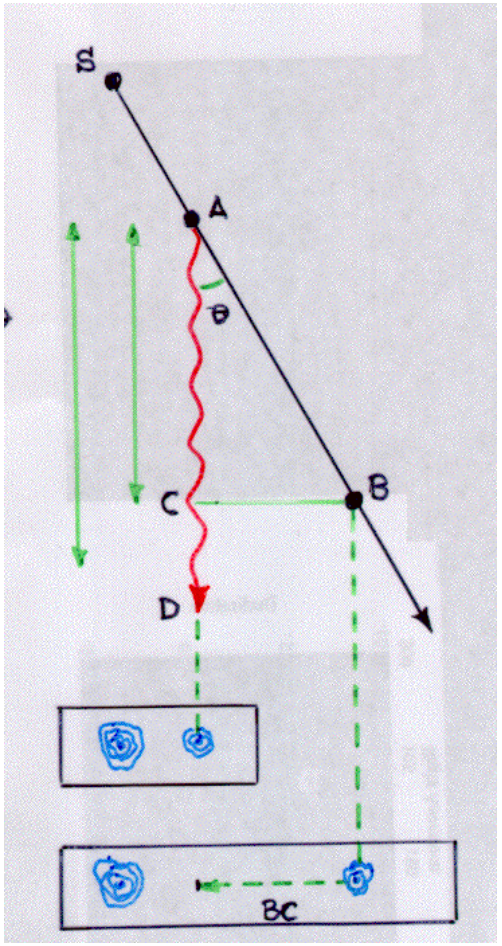

Superluminal motion

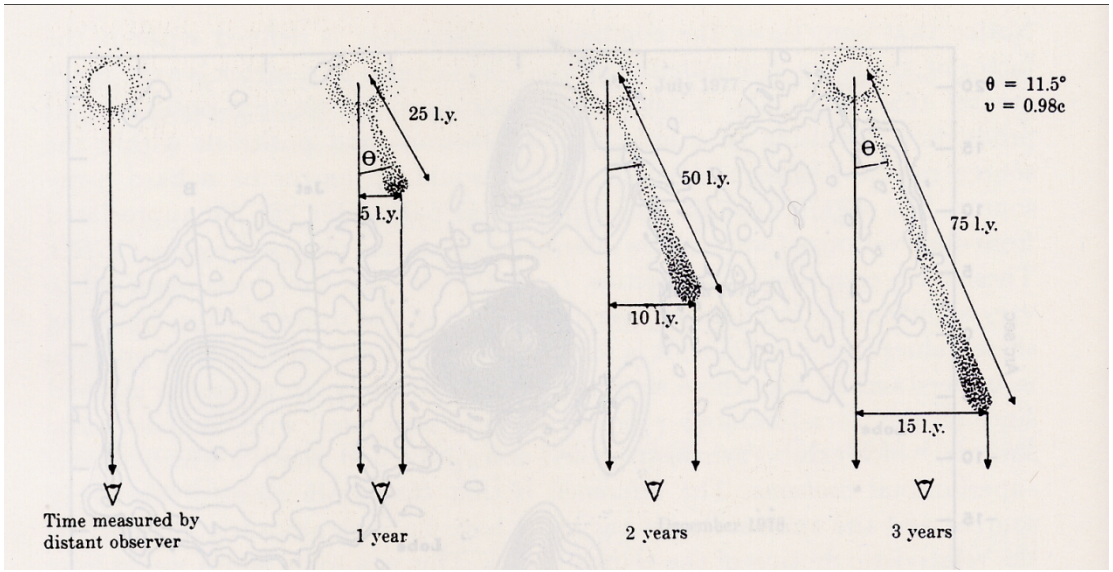

Arrival time of "bullets" emission

$$t_A' = t_A + \frac{D + v\delta t \cos\theta}{c}$$

$$t_B' = t_B + \frac{D}{c}$$

$$\delta t' = \delta t(1 - \beta\cos\theta)$$

$$v_\perp = \frac{v\sin\theta}{1 - \beta\cos\theta}$$

$$\cos\theta = \frac{v}{c}$$

$$\sin\theta = \sqrt{1 - \beta^2}$$

$$v_\perp = \gamma v$$

The compactness problem

$$R_i < c\delta t \qquad \gamma\gamma \rightarrow e^+e^-$$

$$\tau_{\gamma\gamma} = \frac{f_p \sigma_T F D_L^2}{R_i^2 m_e c^2} \approx 10^{17} f_p \left(\frac{F}{10^{-6} erg/cm^2}\right)\left(\frac{D_L}{3Gpc}\right)^2\left(\frac{\delta t}{1ms}\right)$$

$$\tau_{\gamma\gamma} >> 1$$

Very High Optical Depth to pair production

Size

$$R_i < \Gamma^2 c\delta t$$

Pair fraction

$$f_p \rightarrow f_p \Gamma^{-2\alpha}$$

$$\Gamma = \frac{1}{\sqrt{1-\beta^2}}$$

$$\tau_{\gamma\gamma} = \frac{f_p \sigma_T F D_L^2}{R_i^2 m_e c^2} \approx \frac{10^{17}}{\Gamma^{4+2\alpha}} f_p \left(\frac{F}{10^{-6} erg/cm^2}\right)\left(\frac{D_L}{3Gpc}\right)^2\left(\frac{\delta t}{1ms}\right)$$

$$\Gamma \approx 10^2 \div 10^3$$

Piran (1999)

Relativistic motion of the emitting region

Radial transformations

Consider an observer located at a distance R from the point A. The radiation from A reaches the observer at time R/c. The radiation emitted from B takes place at time L/v later and it then travels a distance $(R - L)$ at the speed of light to reach the observer. The trailing edge of the pulse therefore arrives at the observer at a time $L/v + (R - L)/c$. The duration of the pulse as measured by the observer is therefore

$$\Delta t = \left[\frac{L}{v} + \frac{(R-L)}{c}\right] - \frac{R}{c} = \frac{L}{v}\left[1 - \frac{v}{c}\right] . \qquad (8.16)$$

The observed duration of the pulse is much less than the time interval L/v, which might have been expected. Only if light propagated at an infinite velocity would the duration of the pulse be L/v. The intriguing point about this analysis is that the factor $1 - (v/c)$ is exactly the same factor which appears in the Liénard–Wiechert potentials (6.19) and which takes account of the fact that the source of radiation is moving towards the observer. The

Radial transformations

relativistic electron almost catches up with the radiation emitted at A since $v \approx c$, but not quite. We can rewrite (8.16) using the fact that

$$\frac{L}{v} = \frac{r_g \theta}{v} \approx \frac{1}{\gamma \omega_r} = \frac{1}{\omega_g} , \tag{8.17}$$

where ω_g is the non-relativistic angular gyrofrequency and $\omega_r = \omega_g/\gamma$ the relativistic angular gyrofrequency. We can also rewrite $(1 - v/c)$ as

$$\left(1 - \frac{v}{c}\right) = \frac{[1 - (v/c)]\,[1 + (v/c)]}{[1 + (v/c)]} = \frac{\left(1 - v^2/c^2\right)}{1 + (v/c)} \approx \frac{1}{2\gamma^2} , \tag{8.18}$$

since $v \approx c$. Therefore, the observed duration of the pulse is

$$\Delta t \approx \frac{1}{2\gamma^2 \omega_g} . \tag{8.19}$$

Relativistic effects

- **Light aberration:** photons emitted at right angles with respect to the velocity vector (in K') are observed in K to make an angle given by $\sin\theta = 1/\Gamma$. This means that in K half of the photons are concentrated in a cone of semi-aperture angle corresponding to $\sin\theta = 1/\Gamma$.

- **Arrival time of the photons**: as discussed above, the emission and arrival time intervals are different. As measured in the same frame K we have, as before, $\Delta t_a = \Delta t_e(1-\beta\cos\theta)$. If $\Delta t'_e$ is measured in K', $\Delta t_e = \Gamma\Delta t'_e$ leading to

$$\Delta t_a = \Gamma(1-\beta\cos\theta)\Delta t'_e \equiv \frac{\Delta t'_e}{\delta} \tag{2}$$

  Here we have introduced the factor δ, referred to as the beaming or Doppler factor. It exceeds unity for small viewing angles, and if so, observed time intervals are *contracted.*

- **Blueshift/Redshift of frequencies**: since frequencies are the inverse of times, we just have $\nu = \delta\nu'$.

Ghisellini astro-ph/9905181

Relativistic effects

$\nu = \delta\nu'$	frequency
$t = t'/\delta$	time
$V = \delta V'$	volume
$\sin\theta = \sin\theta'/\delta$	sine
$\cos\theta = (\cos\theta' + \beta)/(1 + \beta\cos\theta')$	cosine
$I(\nu) = \delta^3 I'(\nu')$	specific intensity
$I = \delta^4 I'$	total intensity
$j(\nu) = \delta^2 j'(\nu')$	specific emissivity
$\kappa(\nu) = \kappa'(\nu')/\delta$	absorption coefficient
$T_B = \delta T'_B$	brightness temperature (size directly measured)
$T_B = \delta^3 T'_B$	brightness temperature (size from variability)

$\delta = \gamma(1-(V/c)\cos\theta)$

Ghisellini astro-ph/9905181

The Fireball model

- Relativistic motion of the emitting region
- Shock mechanism converts the kinetic energy of the shells into radiation.
- Baryon Loading problem

External Shock
- Synchrotron & SSC
- High conversion efficiency
- Not easy to justify the rapid variability

Internal Shocks
- Source activity
- Synchrotron Emission
- Rapid time Variability
- Low conversion efficiency

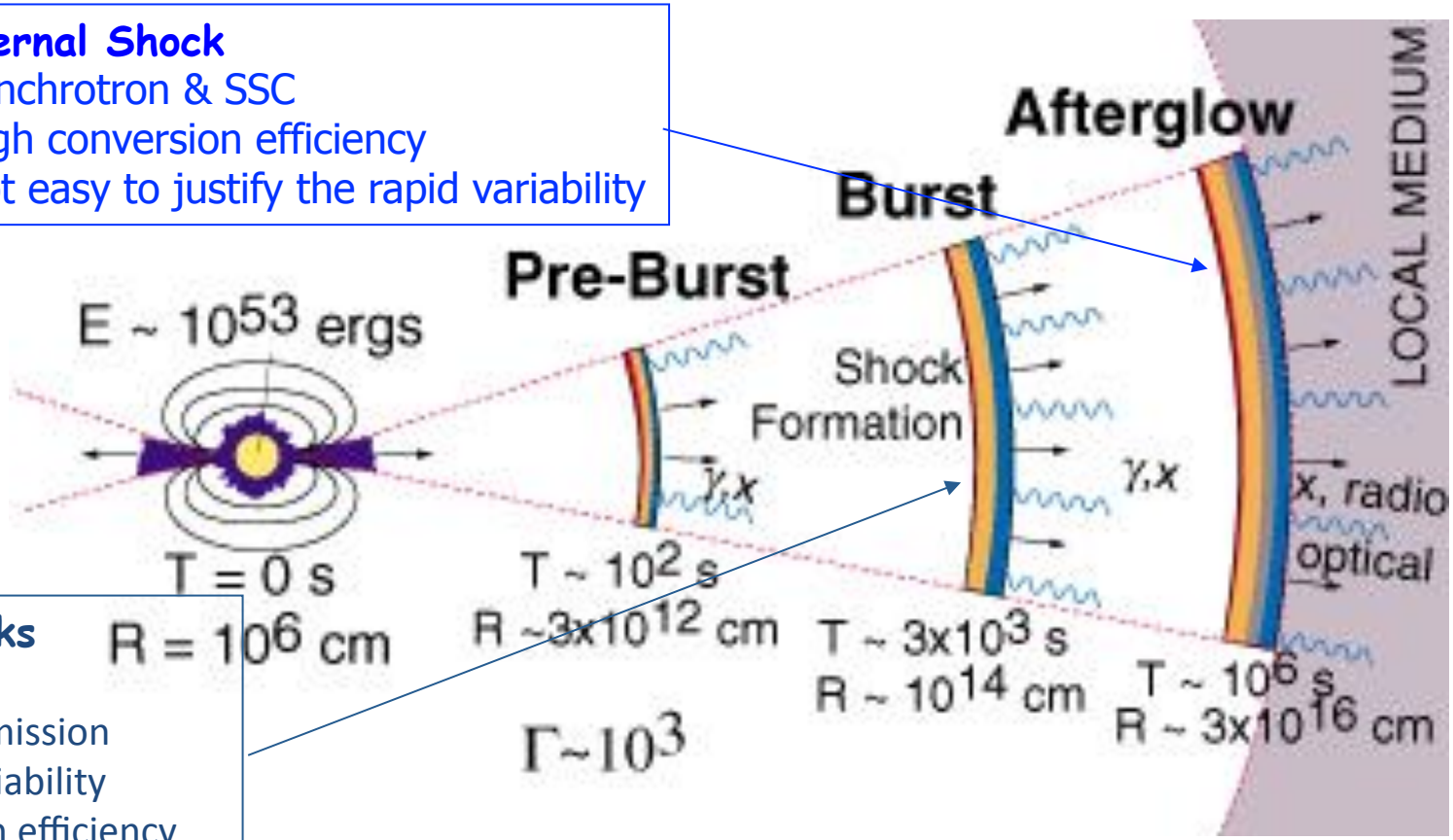

Afterglow Observations

Harrison et al (1999)

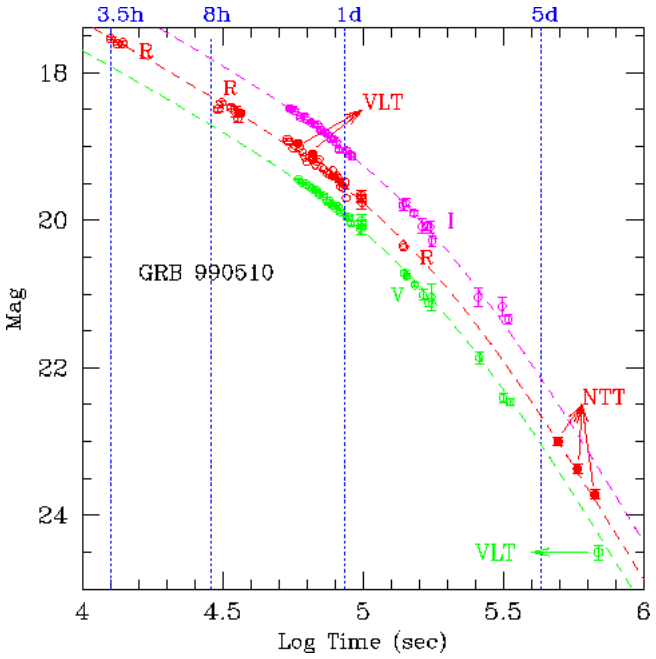

Achromatic Break

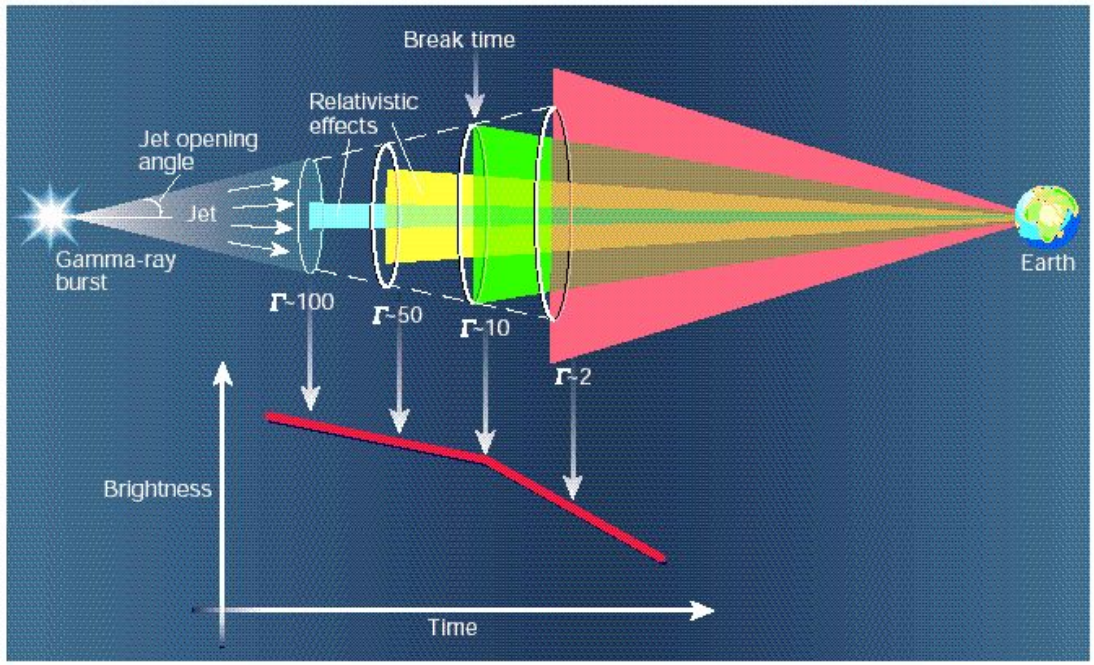

Woosley (2001)

Jet and Energy Requirements

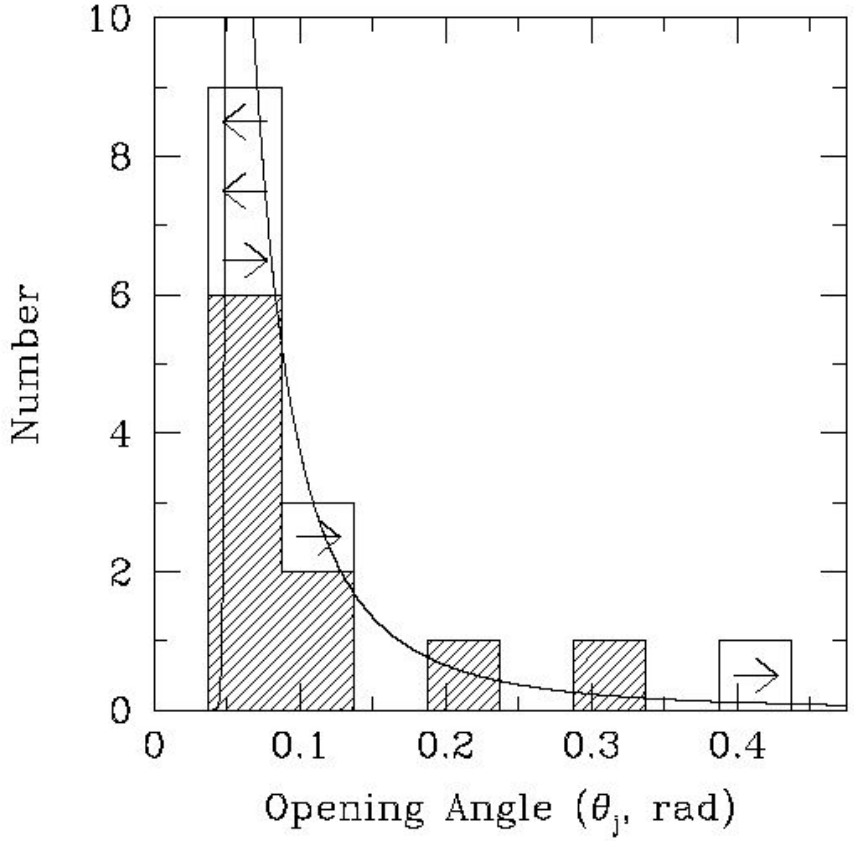

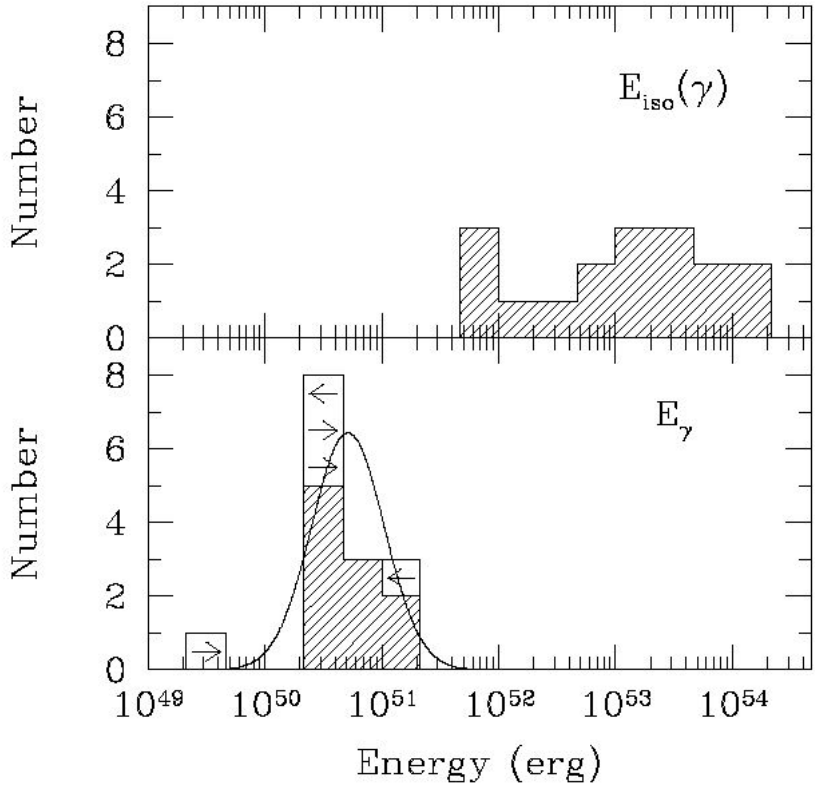

Frail et al. (2001)

Relativistic beaming

Suppose two frames are moving relative to each other with velocity **v** along the z-axis. Then, according to equation (3.10), the component $u_z = dz/dt$ of a velocity u measured in the laboratory frame is

$$\frac{dz}{dt} = \frac{dz' + v\,dt'}{dt' + v\,dz'/c^2} \tag{5.87}$$

or

$$u_z = \frac{u'_z + v}{1 + vu'_z/c^2}. \tag{5.88}$$

Similarly, in the (x- or) y-direction,

$$u_y = \frac{dy}{dt} = \frac{dy'}{\gamma(dt' + v\,dz'/c^2)}, \tag{5.89}$$

which also simplifies to the form

$$u_y = \frac{u'_y}{\gamma(1 + vu'_z/c^2)}. \tag{5.90}$$

Since we wish to determine boosting effects relative to **v**, let us define the angle $\psi \equiv \pi/2 - \theta$. Then, using this angle convention with $u = c$, we infer from

Relativistic beaming

equation (5.90) that

$$\sin\psi = \frac{\sin\psi'}{\gamma(1+\beta\cos\psi')}. \tag{5.91}$$

A ray leaving the electron in a direction $\theta' = \pi/4$ to $\ddot{\mathbf{d}}$ has a $dP'/d\Omega'$ equal to half its maximum possible value (which occurs at $\theta' = \pi/2$). However, as seen in the laboratory frame, this ray points in a direction much closer to $\mathbf{v}$. According to equation (5.91),

$$\sin\psi \approx \psi \approx \frac{1}{\gamma}. \tag{5.92}$$

Thus, whereas the power is radiated nearly isotropically in the particle's rest frame, most of it is *beamed* into a narrow cone with half-opening angle $\sim 1/\gamma$ as seen in the laboratory (see also figure 5.8).

Jet breaks

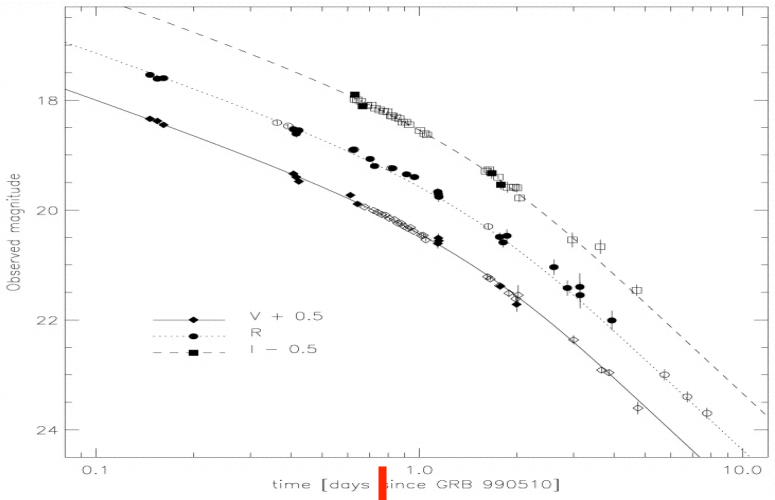

➢ breaks in the afterglow decay light curves -> collimation ?

$$\theta = 0.09 \left(\frac{t_{jet,d}}{1+z}\right)^{3/8} \left(\frac{n\,\eta_\gamma}{E_{\gamma,iso,52}}\right)^{1/8}$$

$$E_\gamma = (1-\cos\theta) E_{\gamma,iso}.$$

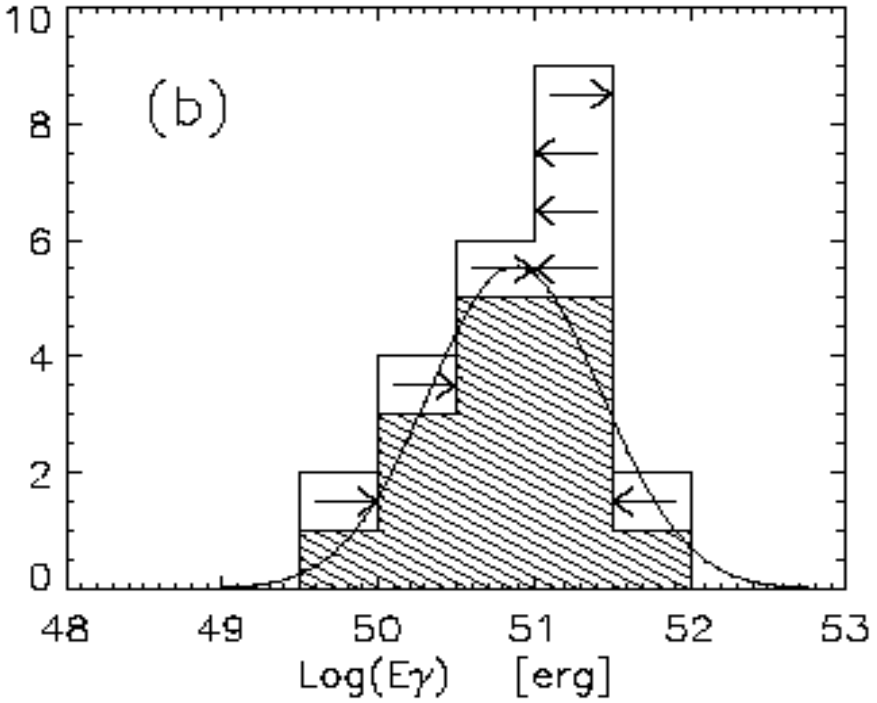

Progenitors

- Two populations of GRB?
- Main models
- Possible solution?

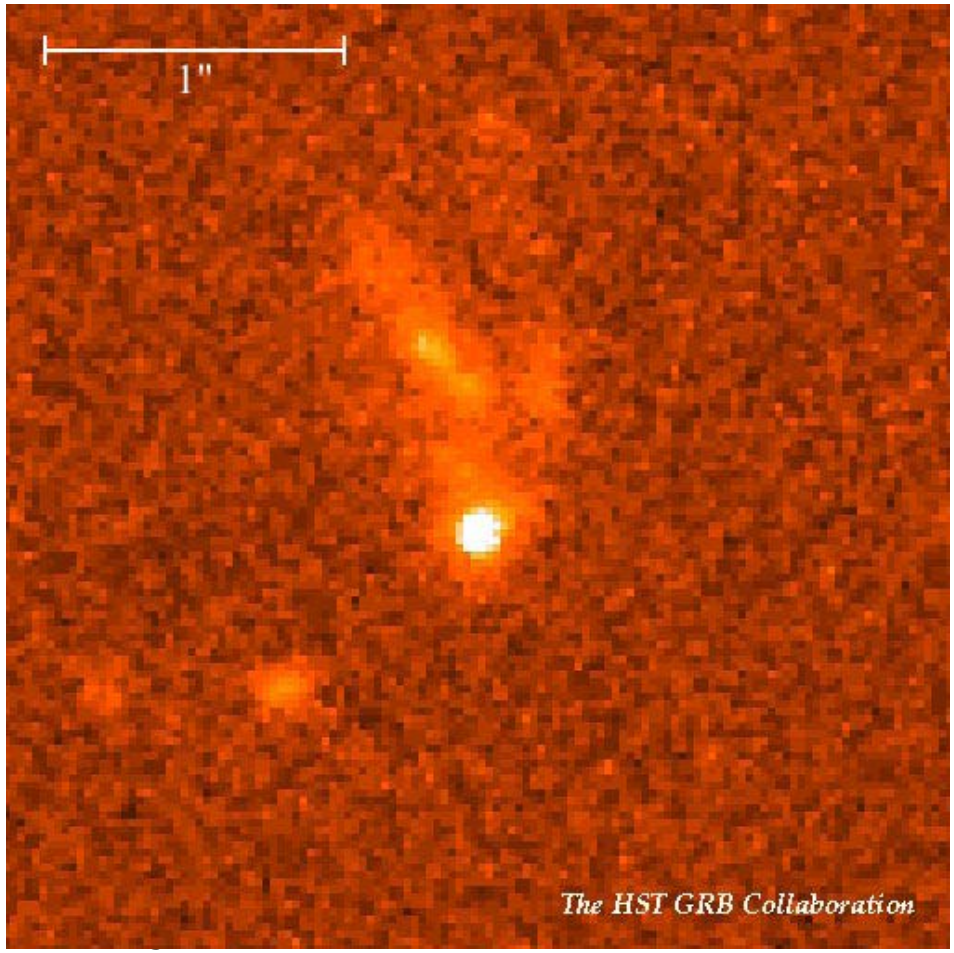

Progenitors

Long GRB

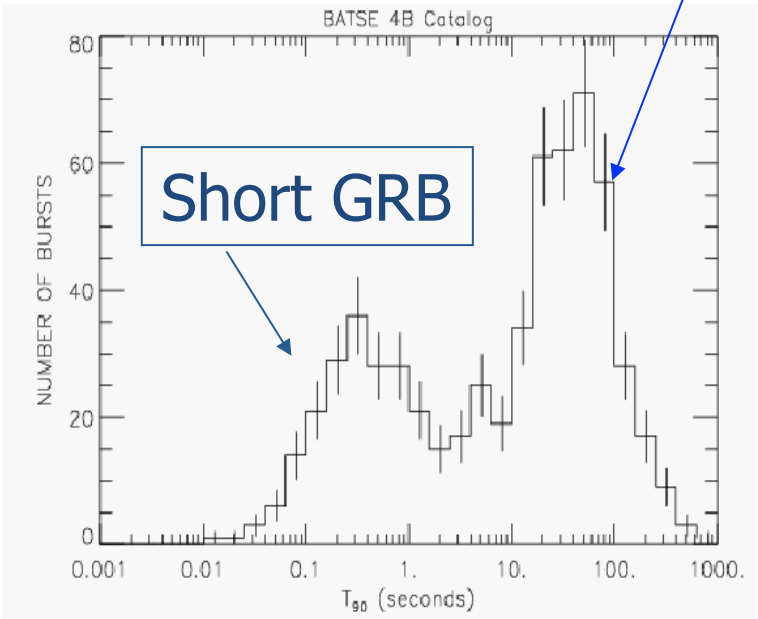

Short GRB

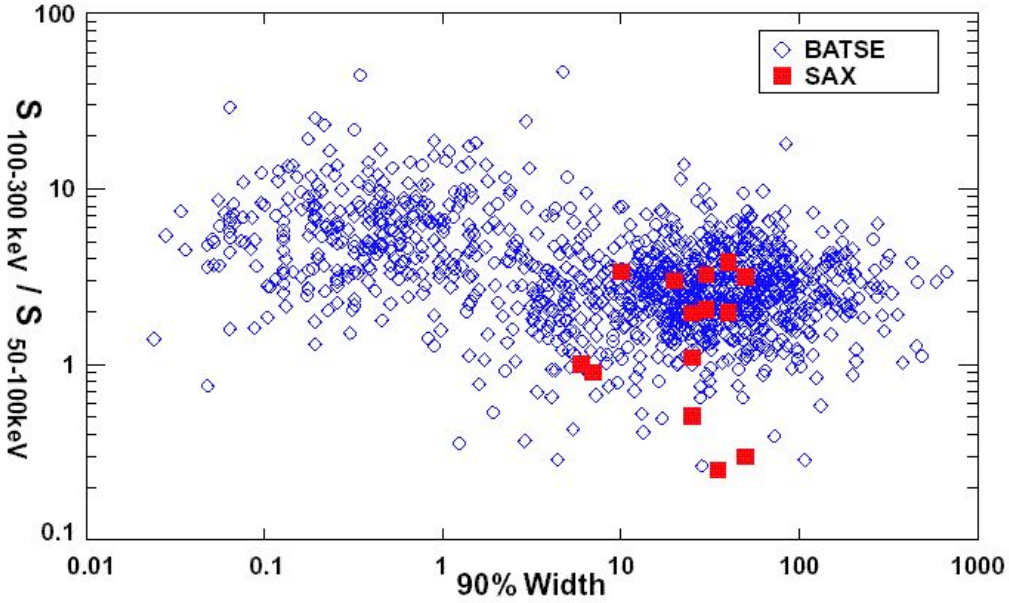

Towards a solution?

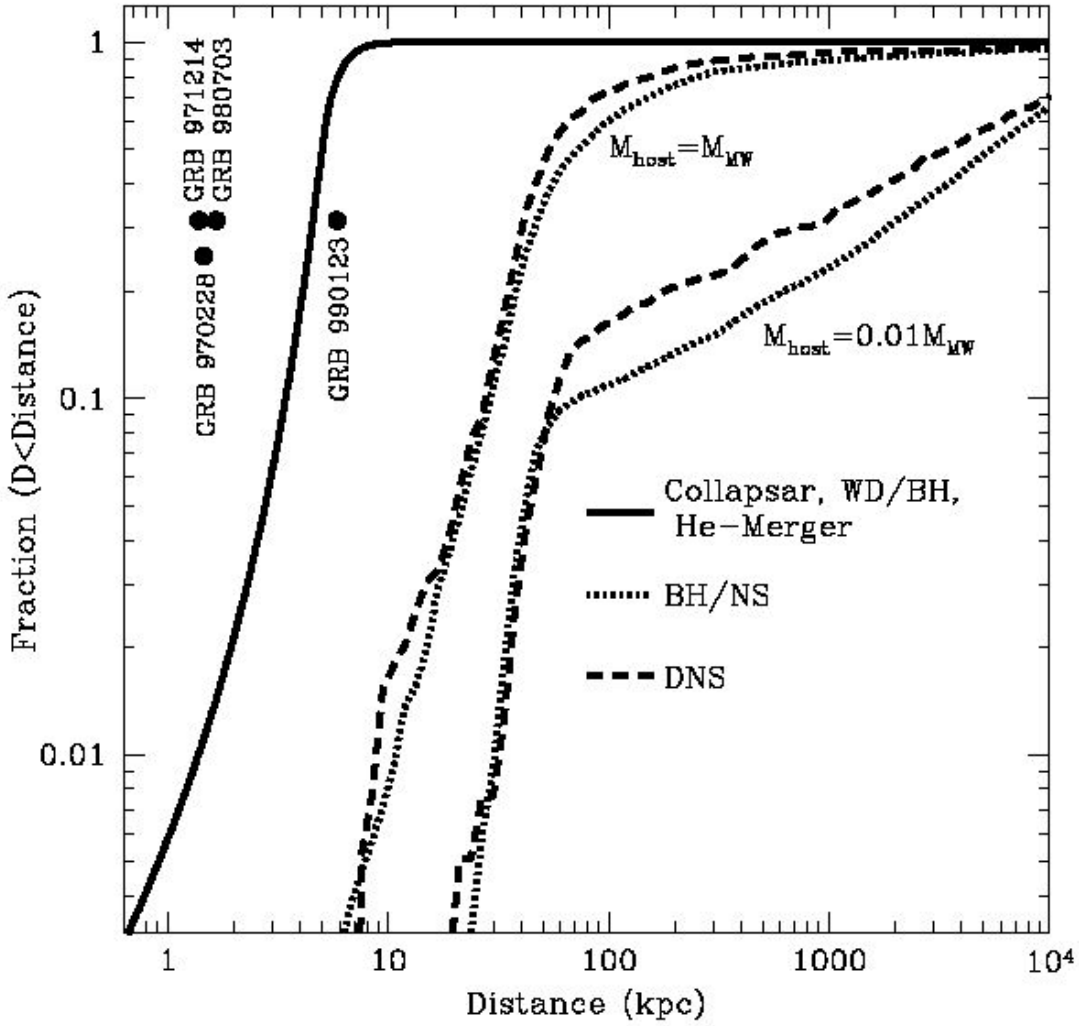

Fryer et al. (1999)

Distance from Host Galaxy

SN- GRB connection

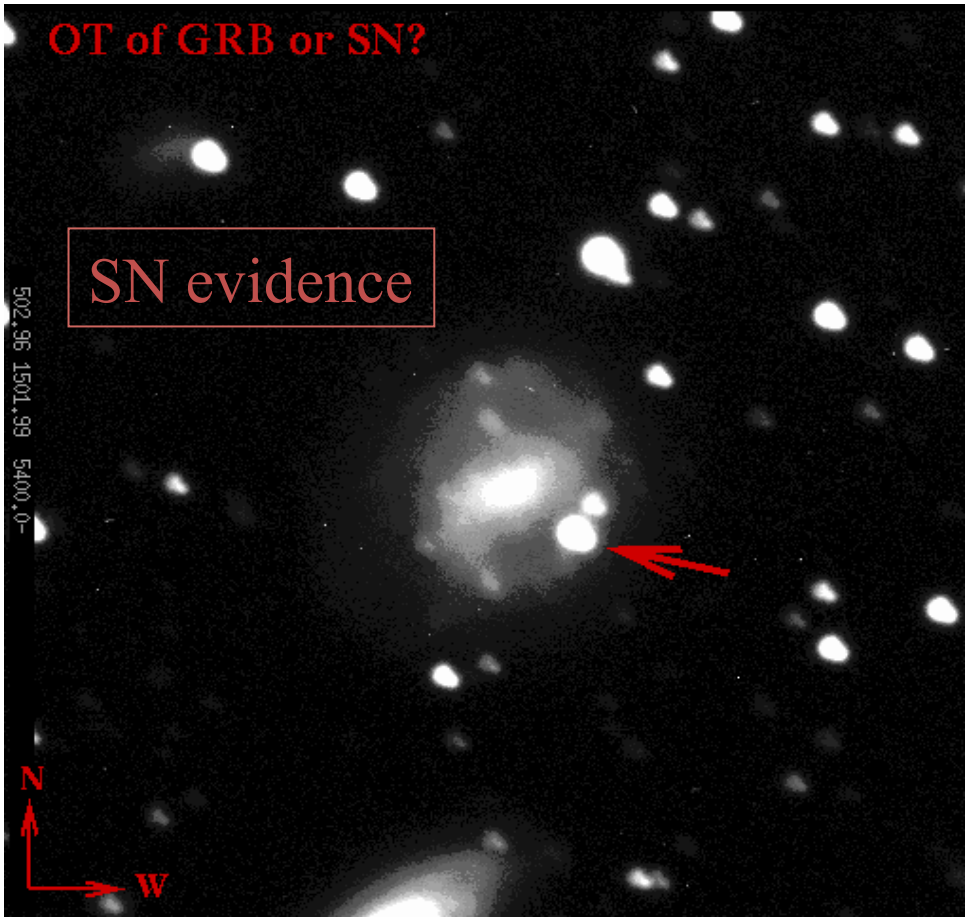

SN 1998bw - GRB 980425
chance coincidence O(10^{-4})
(Galama et al. 98)

GRB & SN first predictions

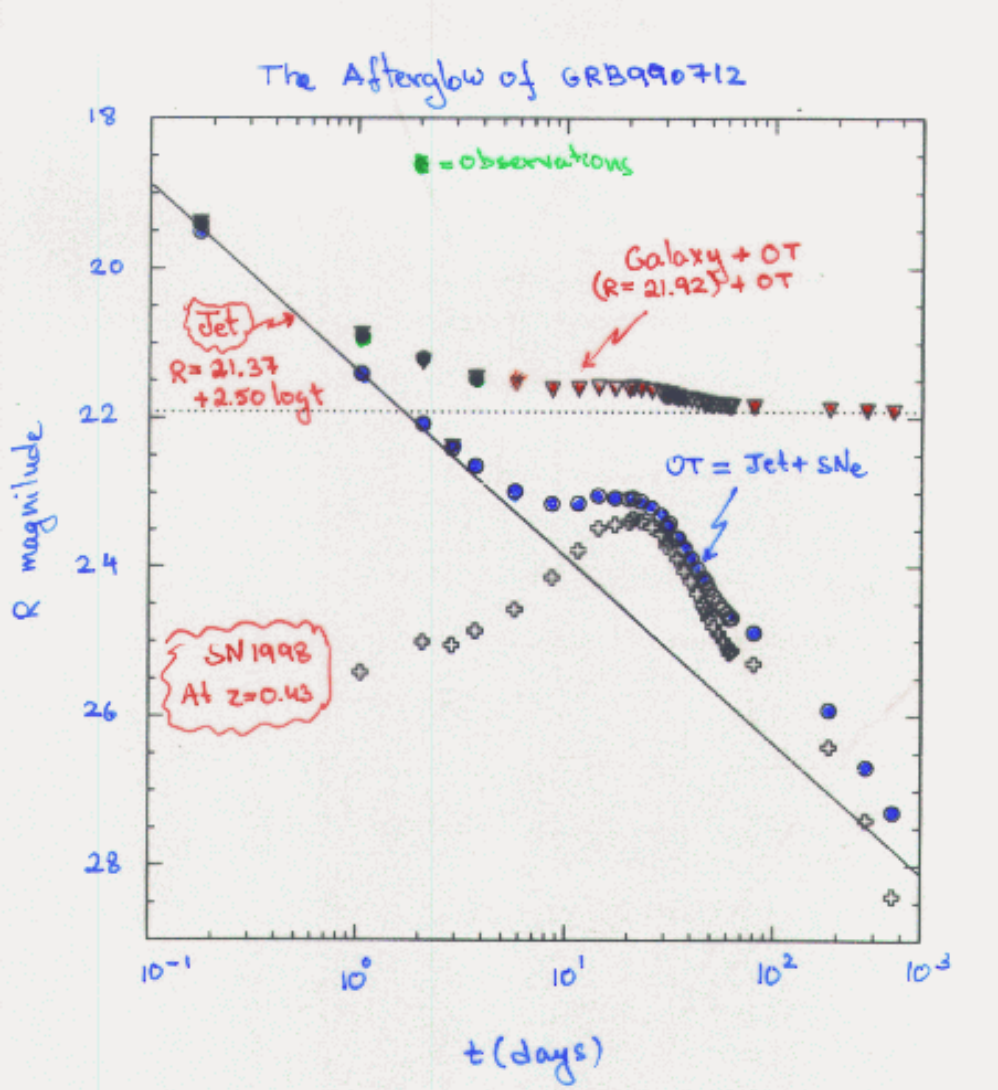

Hjorth, Fynbo, Dar & Courbin (1999)

GRB & SN

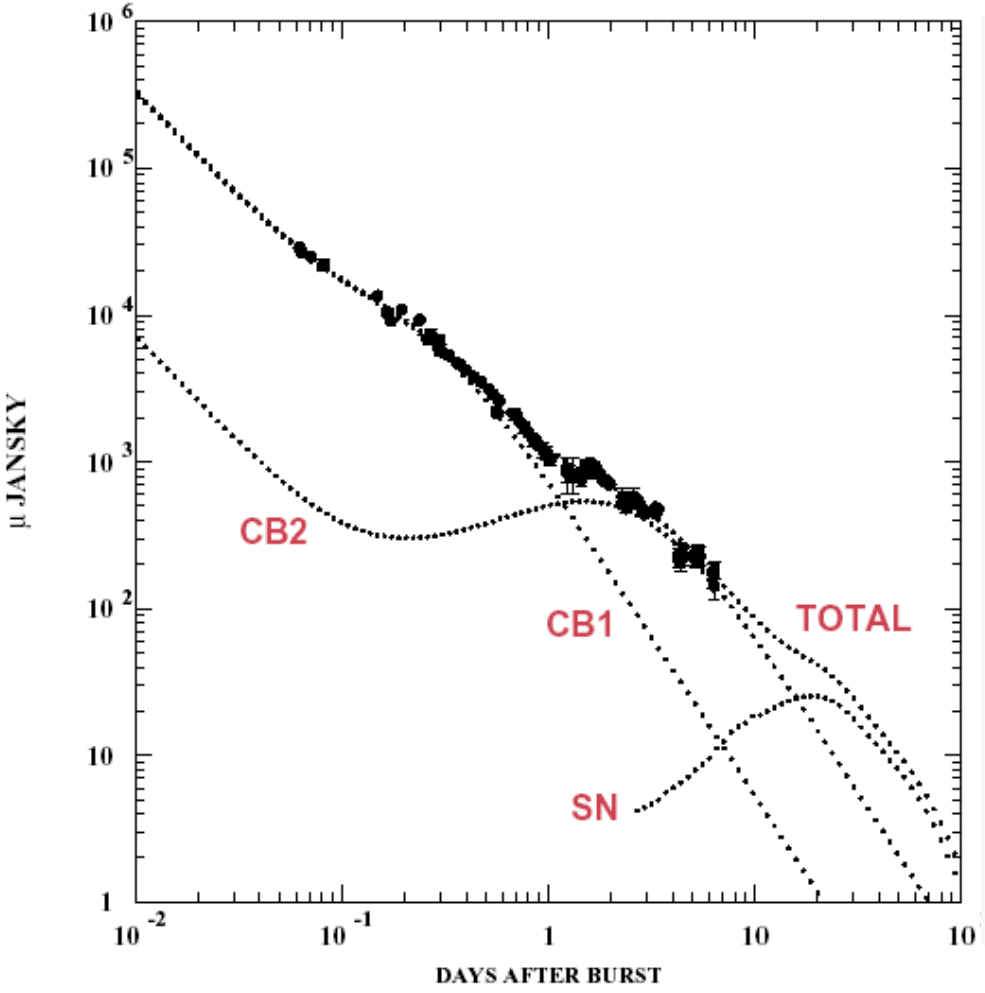

Dado, Dar & De Rujula (2003)

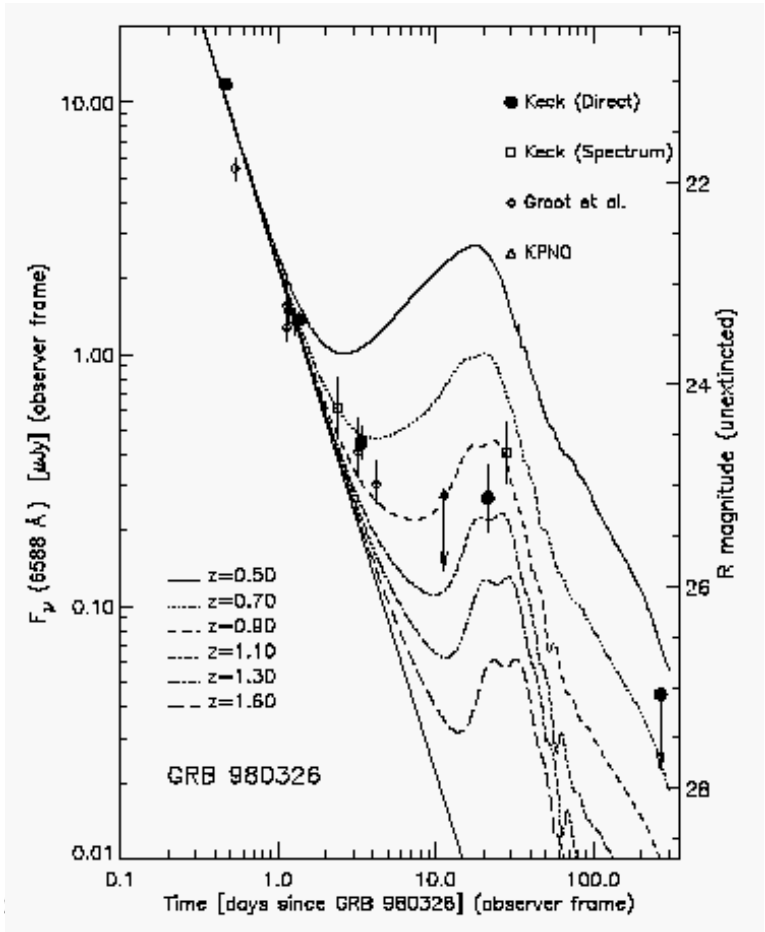

GRB 980326

(Bloom et al. 99)

Hete2

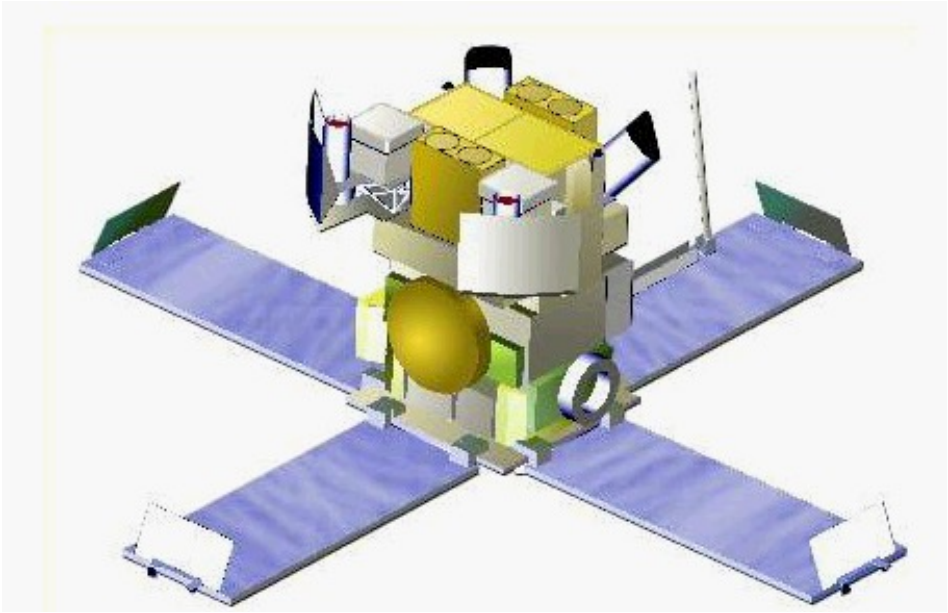

2000 - 2008

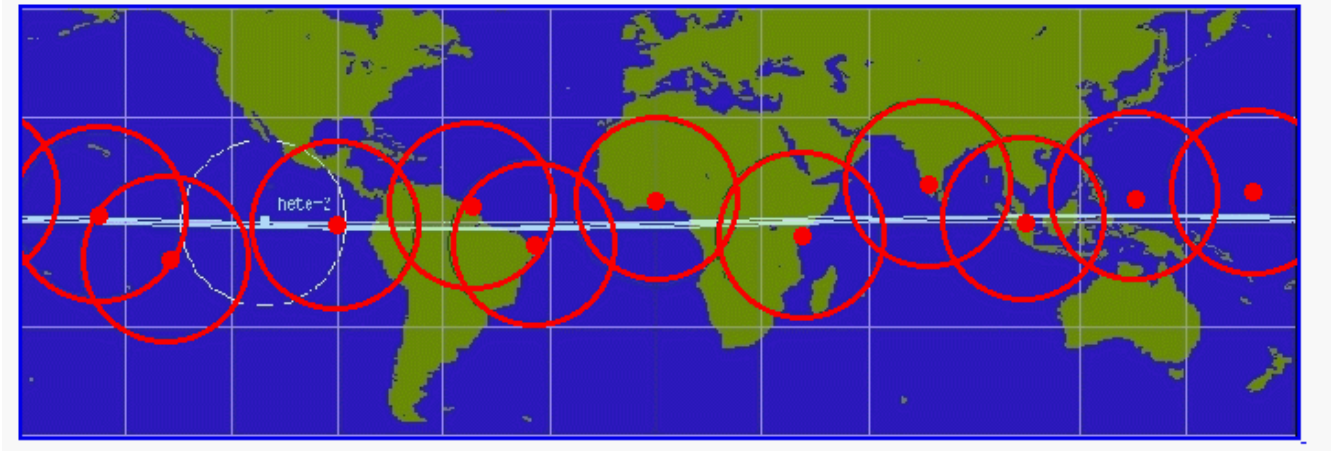

HETE-2 Science Instrument Package

French Gamma-ray Telescope **(FREGATE):** 5-500 keV; ~π FOV

Wide-Field X-ray Monitor **(WXM):** 2-25 keV; ~5'-10' localizations

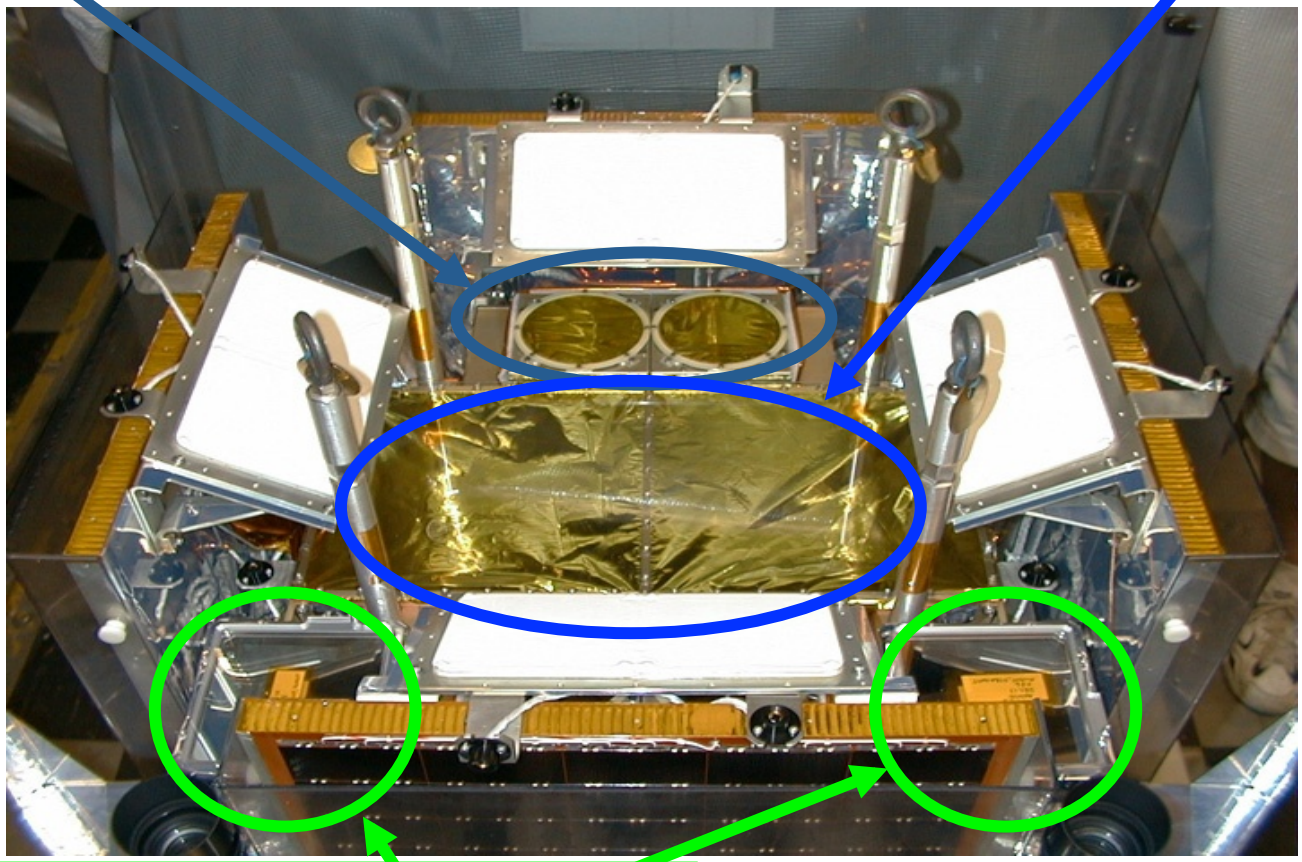

Soft X-ray Cameras **(SXC):**

1-10 keV; ~30" localizations

Hete-II results

- The discovery of GRB 030329 -- connecting GRBs with supernovas.
- The discovery of GRB 050709 -- the first short/hard GRB with optical afterglow -- the cosmological origin of this subclass of GRBs.
- Dark bursts…. Some of these dark GRBs fade in the optical very rapidly, others are dimmer but detectable with large (meter class) telescopes.
- The establishment of another subclass of GRBs, the less energetic X-Ray Flashes (XRF), and its first optical counterpart.
- The first to send out arcminute positions of GRBs to the observation community within tens of seconds of the onset of GRB (and in a few instances, while the burst was ongoing).

GRB050709

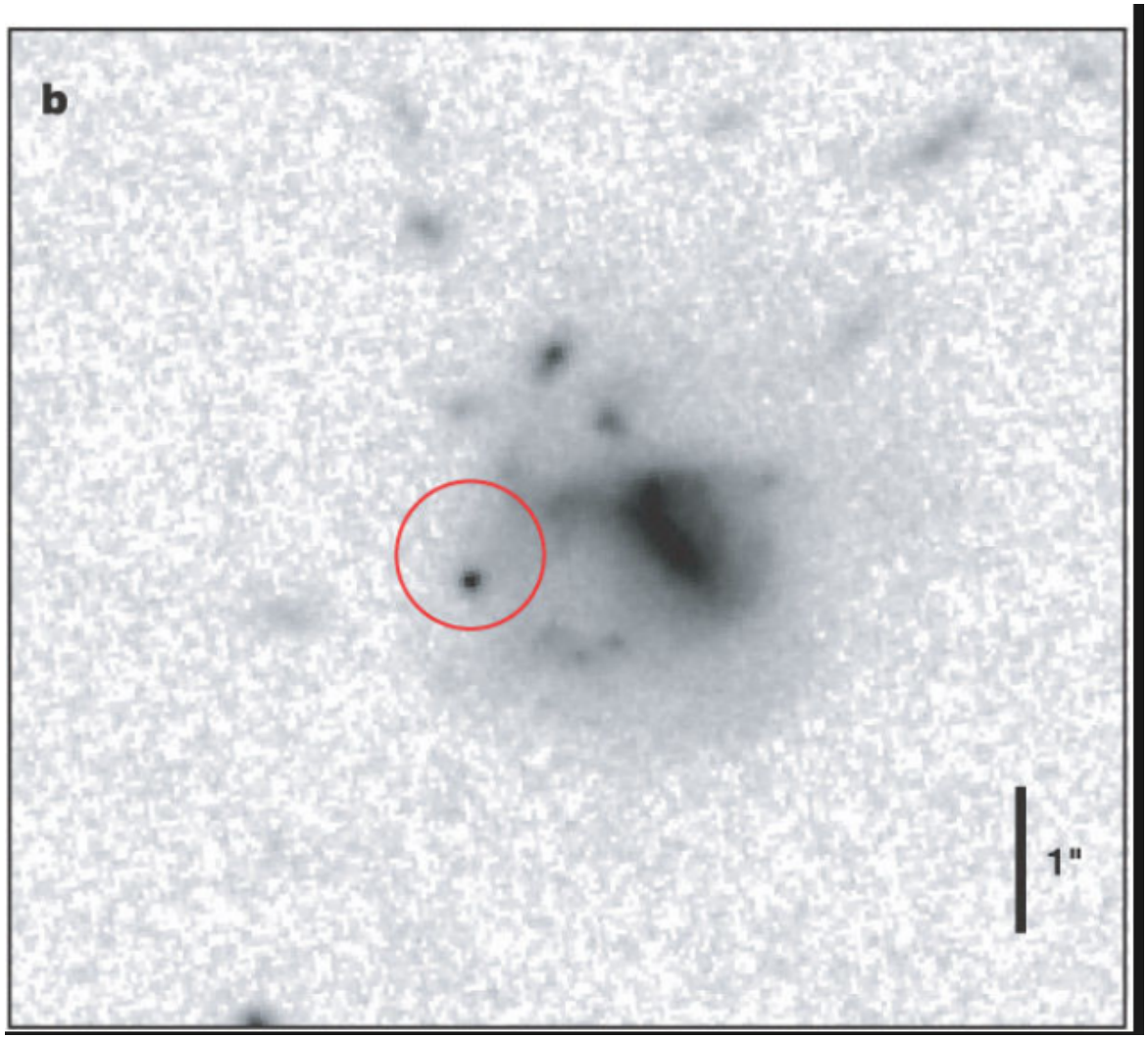

(Fox et al. 2005)

GRB 030329: the "smoking gun"?

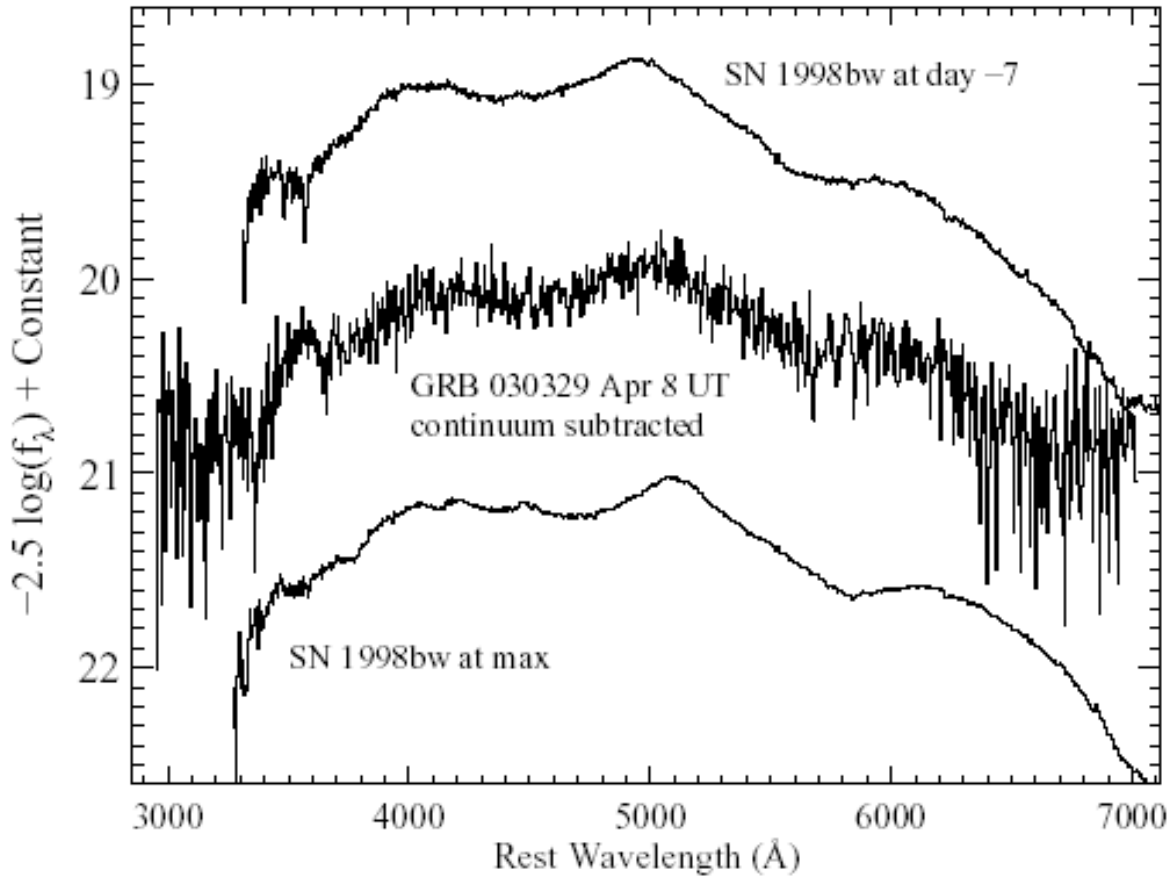

(Matheson et al. 2003)

Collapsar model

Woosley (1993)

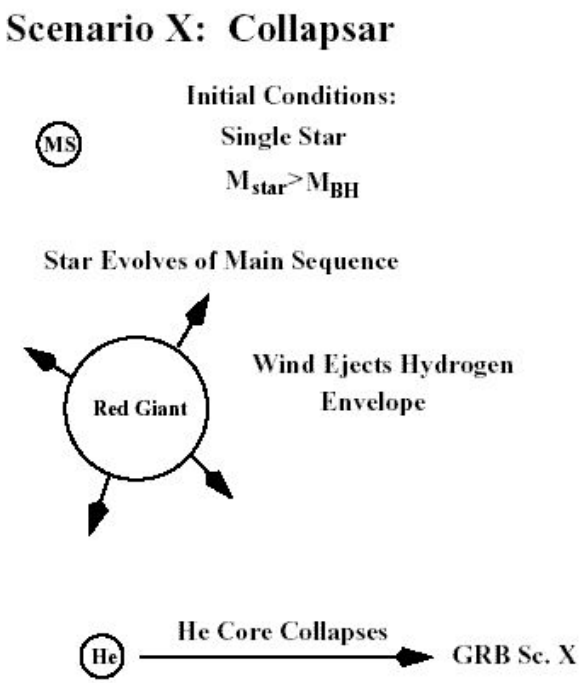

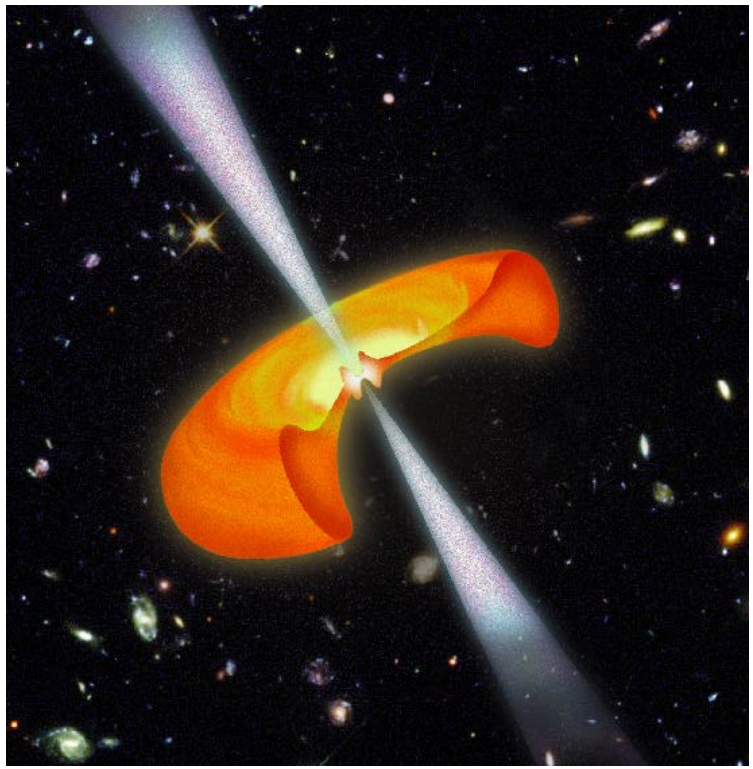

- Very massive star that collapses in a rapidly spinning BH.
- Identification with SN explosion.

Classificazione delle SNe

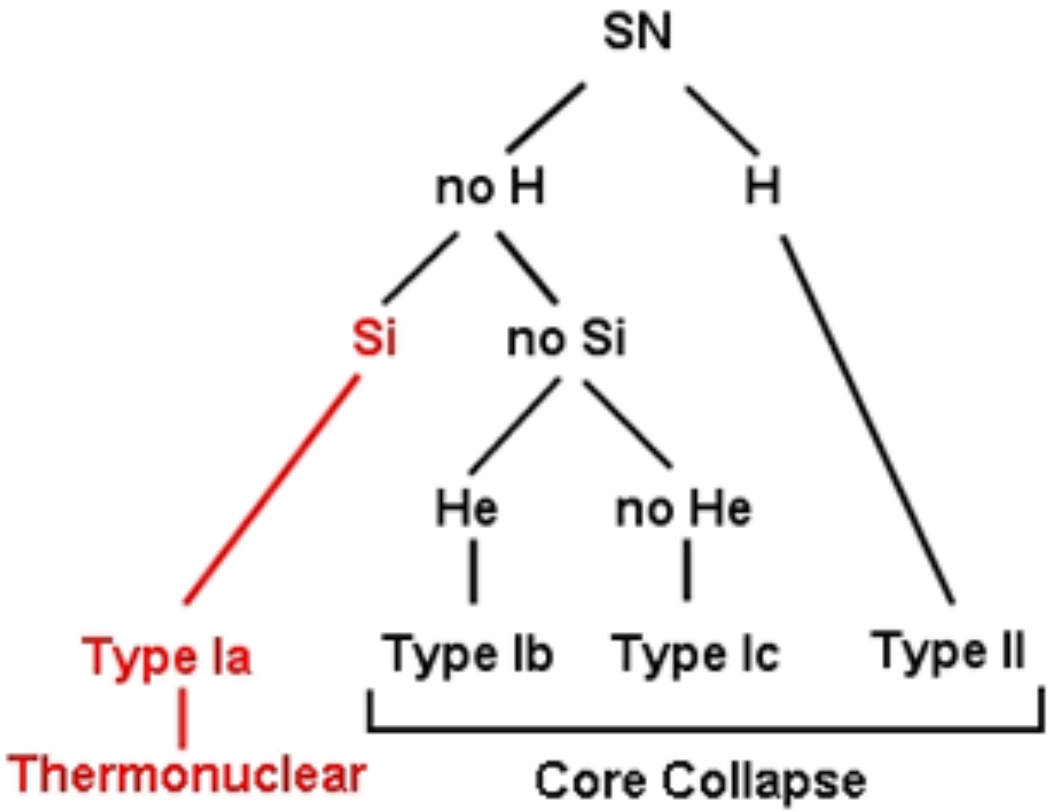

Classificazione delle SNe

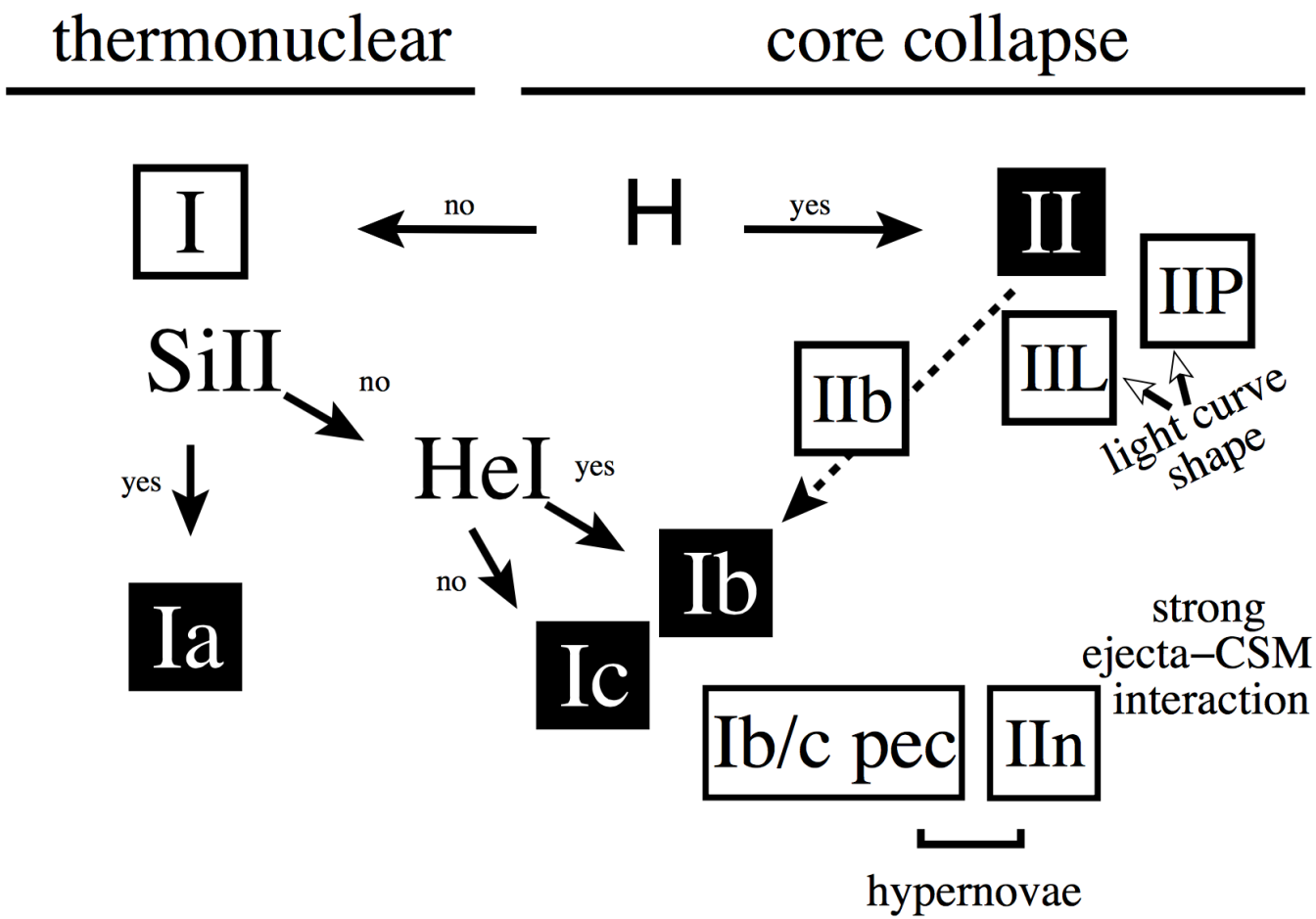

GRBs and Gravitational Waves

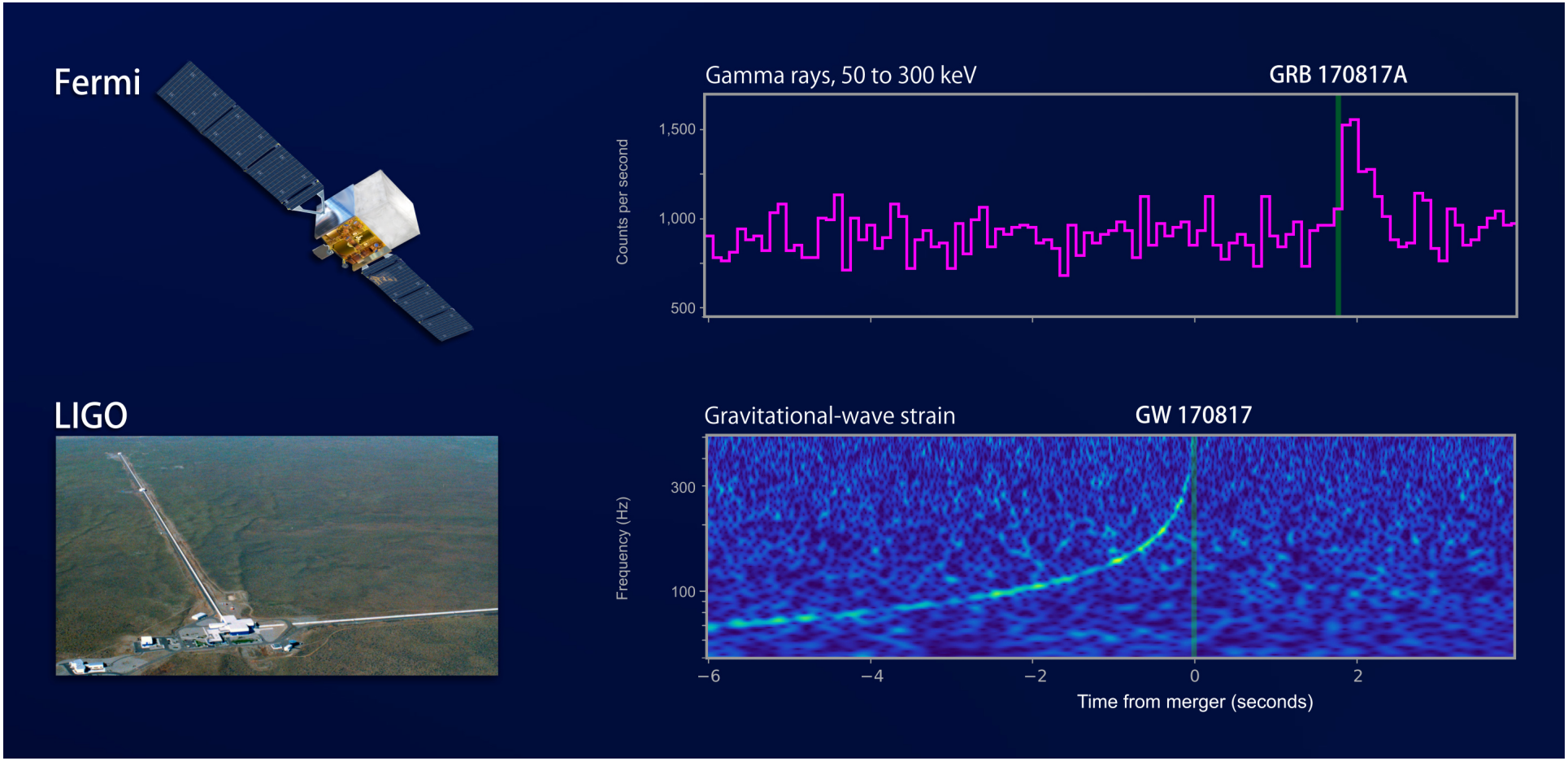

GRBs and Gravitational Waves

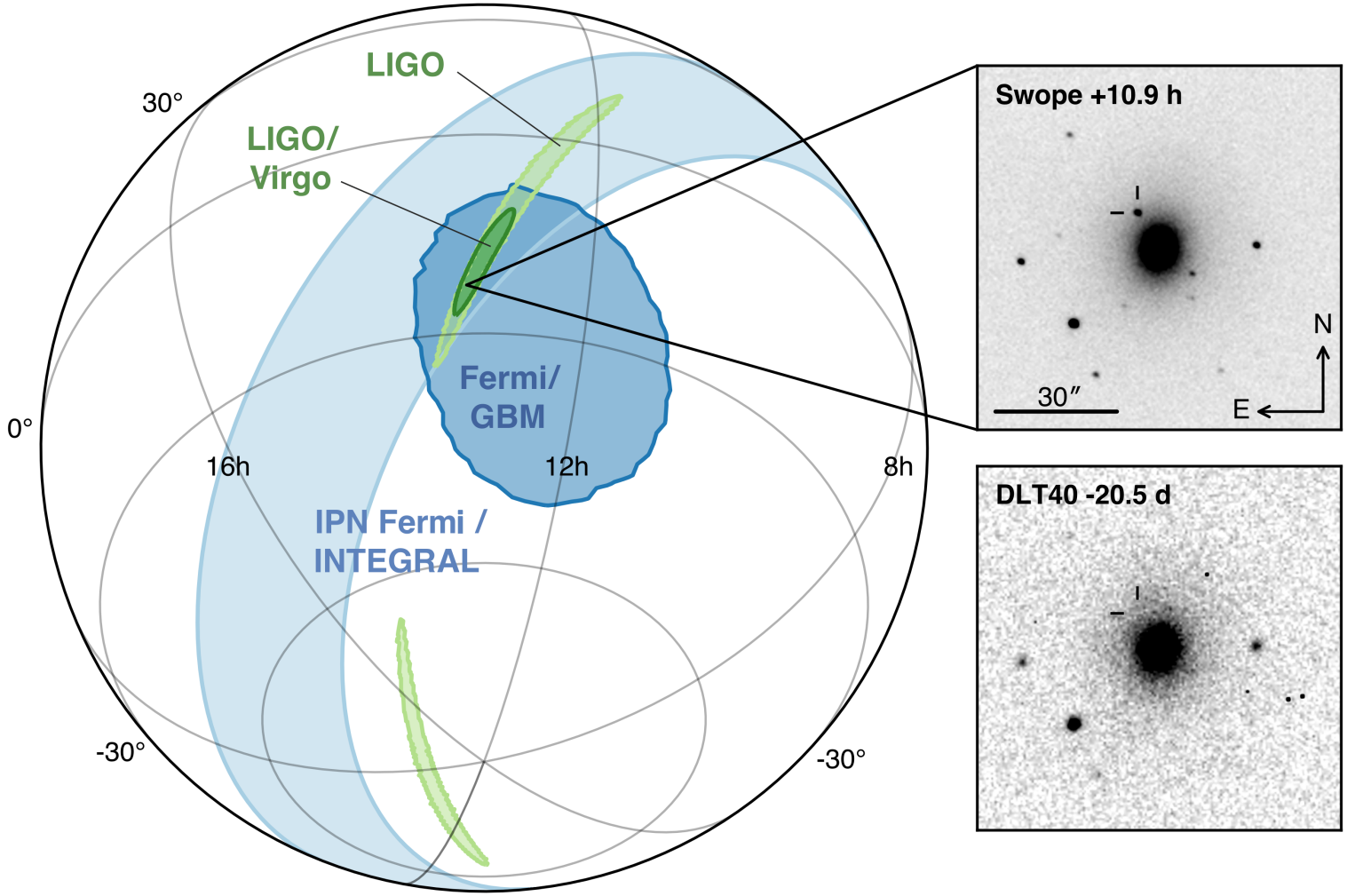

NS/BH Binary Mergers

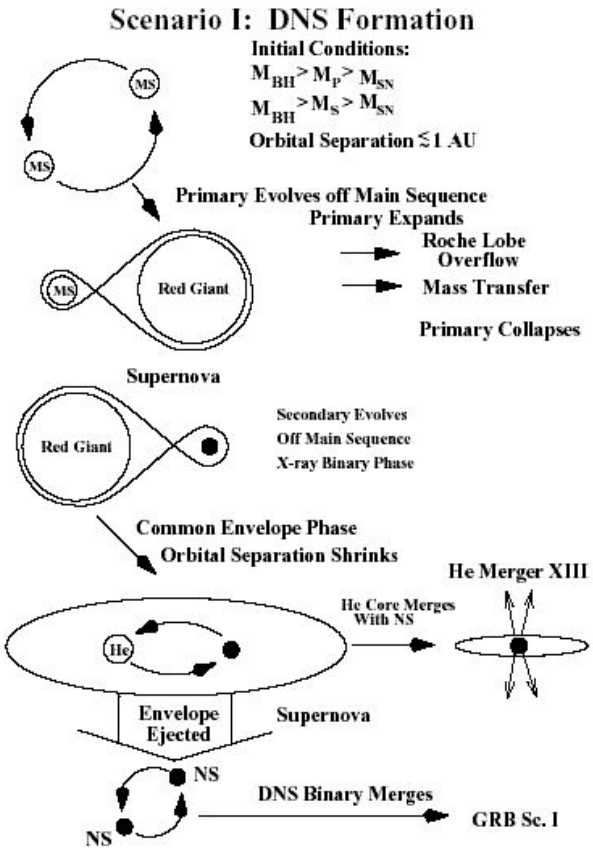

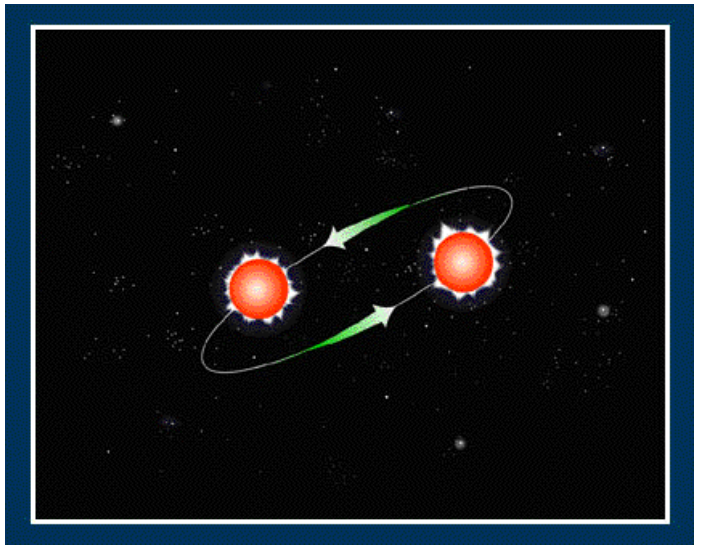

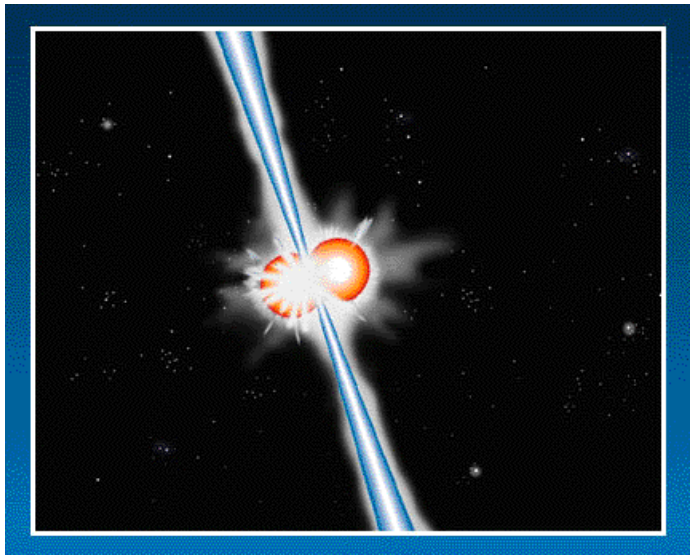

Merging of compact objects (NS-NS, NS-BH, BH-BH).
These objects are observed in our Galaxy.
The merging time is about 10^8 yr, via GW emission.

Eichler et. al. (1989)

Black-Hole Accretion Disk (BHAD) Models

Binary merger or Collapse of rotating Star produces Rapidly accreting Disk (>0.1 solar Mass per second!) Around black hole.

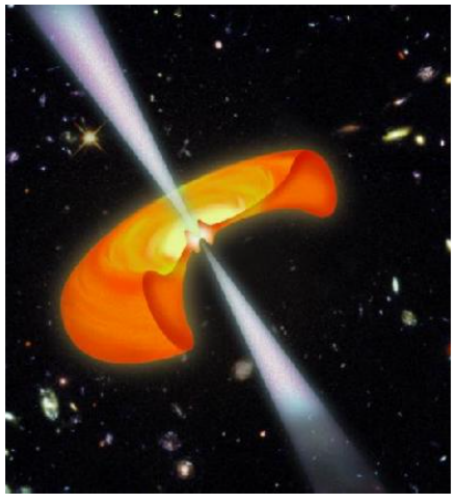

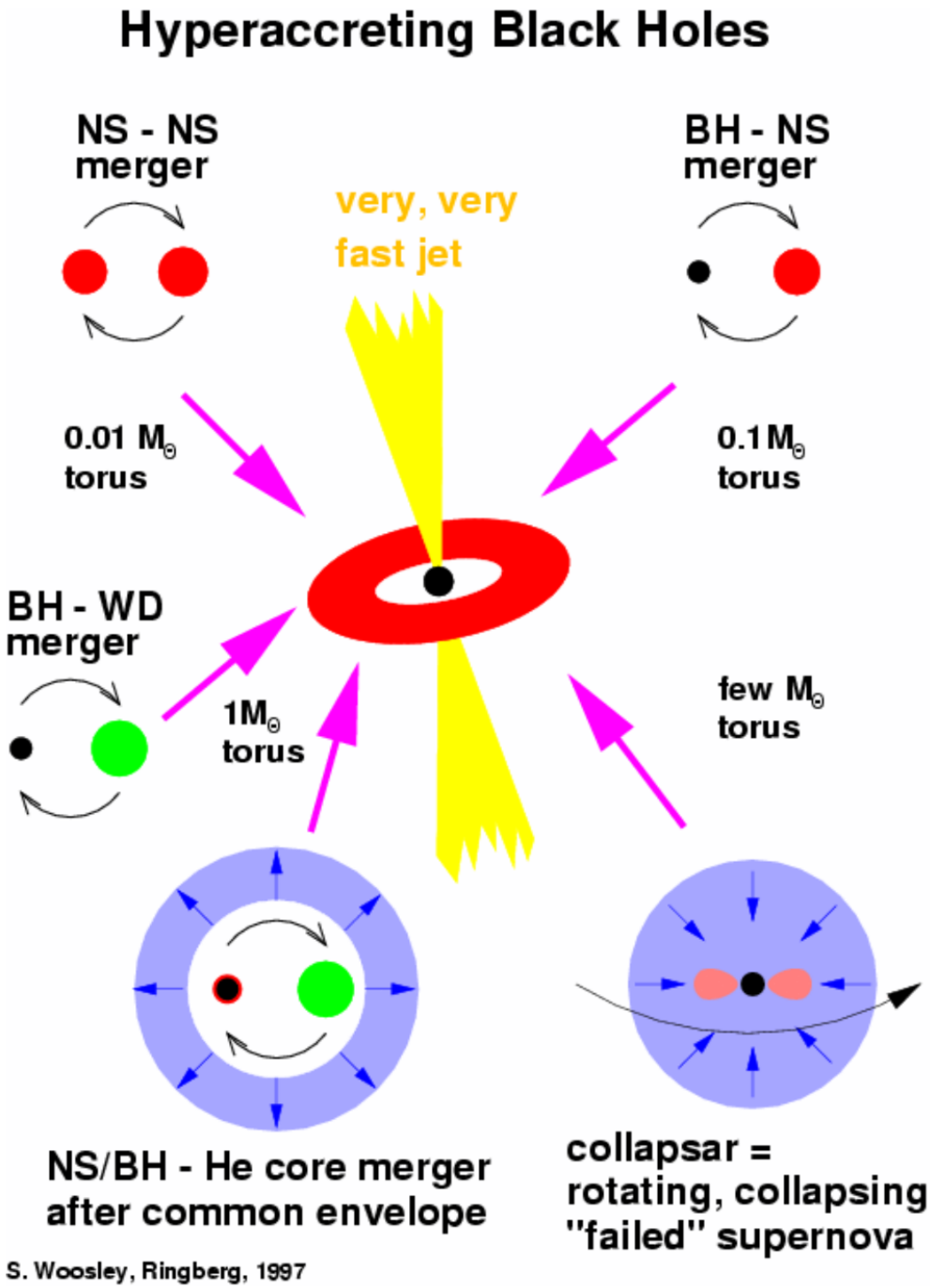

SWIFT

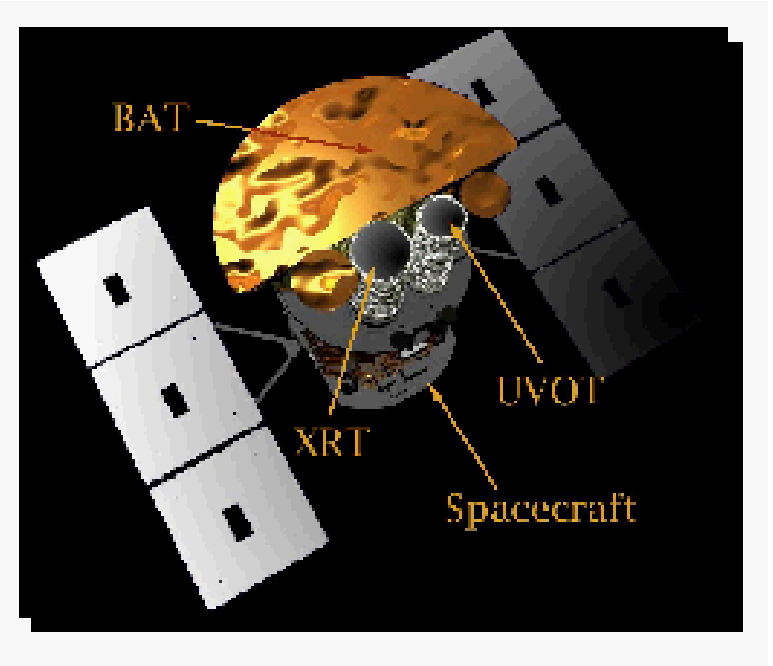

In orbita dal 2004

Swift Instruments

Instruments

- Burst Alert Telescope (BAT)
  - New CdZnTe detectors
  - Most sensitive gamma-ray imager ever
- X-Ray Telescope (XRT)
  - Arcsecond GRB positions
  - CCD spectroscopy
- UV/Optical Telescope (UVOT)
  - Sub-arcsec positions
  - Grism spectroscopy
  - 24th mag sensitivity (1000 sec)
  - Finding chart for other observers

Spacecraft

- Autonomous re-pointing, 20 - 75 s
- Onboard and ground triggers

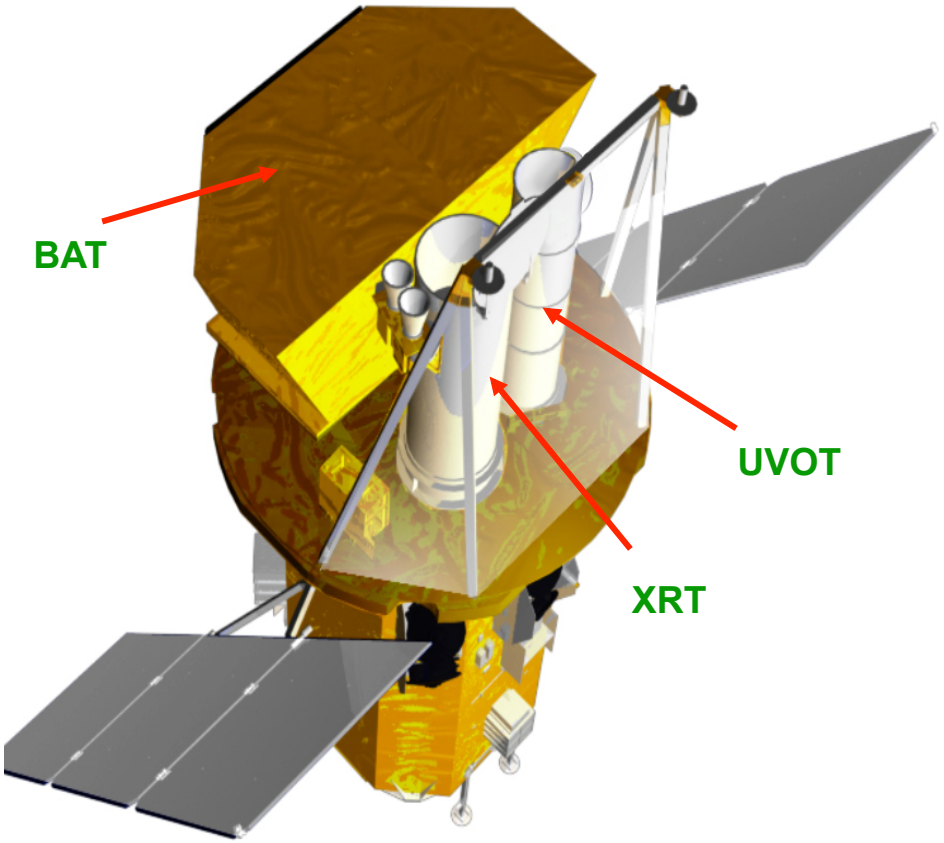

SWIFT

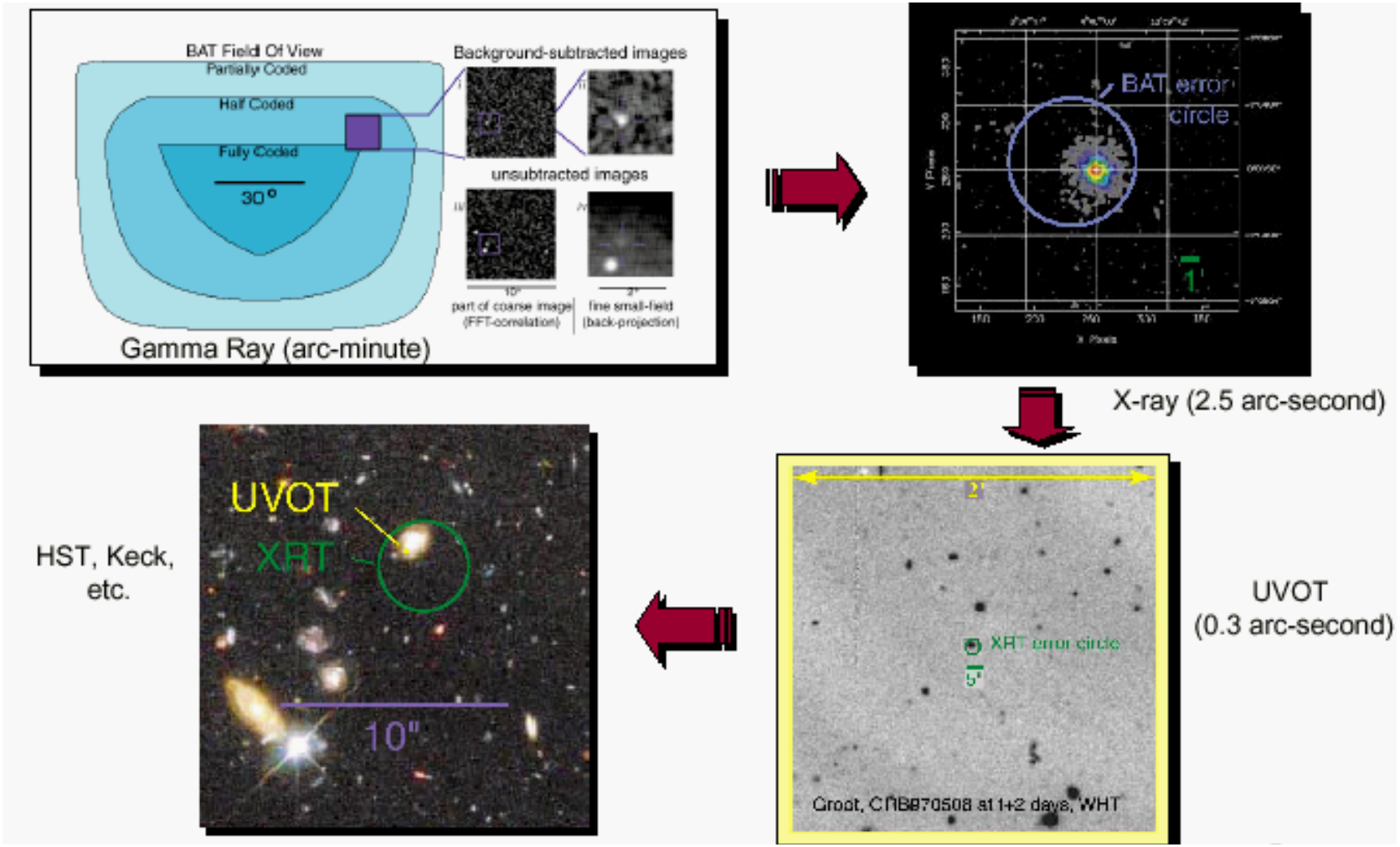
BAT Field Of View
Partially Coded
Half Coded
Fully Coded
30°
Background-subtracted images
unsubtracted images
part of coarse image (FFT-correlation)
fine small-field (back-projection)
Gamma Ray (arc-minute)
BAT error circle
1'
X-ray (2.5 arc-second)
2'
XRT error circle
5'
Groot, CfB970508 at 1+2 days, WHT
UVOT
(0.3 arc-second)
HST, Keck, etc.
UVOT
XRT
10"

Mission Capabilities

Multiwavelength observations on all time scales

>100 GRBs per year of all types

BAT sensitivity 2 - 5 time better than BATSE

Arcsec positions & counterparts for 100's GRBs

Rapid GRB notifications via GCN

Identification of host galaxies offsets

X-ray and UV/optical spectroscopy

Upload capability to slew to GRB and transients detected by other observatories

BAT

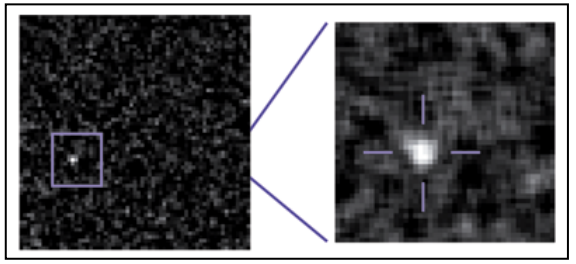

XRT

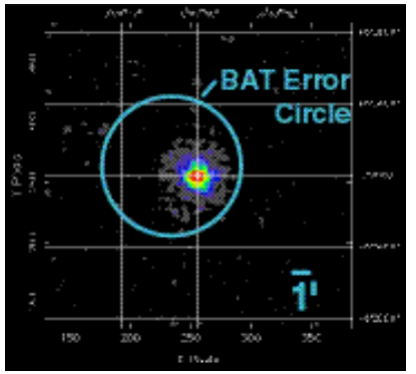

UVOT

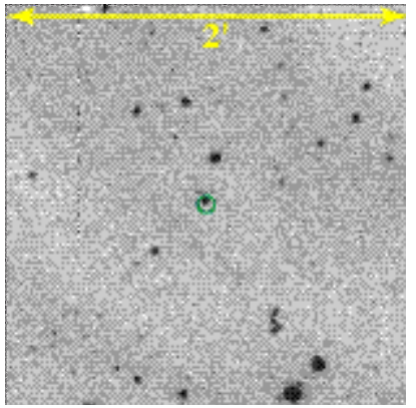

Swift Observatory in Goddard Clean Room